

**Effects of Temperature and Solvent  
Activity on the Viscoelastic Response of  
Nafion<sup>®</sup> for PEM Fuel Cells**

Christine Ranney

An Undergraduate Thesis

Presented to Professor Jay Benziger

Princeton Chemical Engineering Department

April, 2007

*To Barclay*

# Abstract

This thesis will investigate the mechanical properties of Nafion<sup>®</sup>, specifically with respect to viscoelastic creep and membrane swelling, under a range of temperatures and solvent activities. Studies have shown that the mechanical properties of the membrane are extremely important to the performance and longevity of the fuel cell. This paper will focus on a relatively new Polymer Electrolyte Membrane fuel cell (PEM) fuel cell technology, the Direct Methanol Fuel Cell (DMFC). Nafion<sup>®</sup>, a perfluorinated ionomer, is the most commonly used membrane in these fuel cells.

Nafion<sup>®</sup> is a viscoelastic material, which means that it responds to stress in a time-dependant manner. The membrane of a fuel cell is subject to various stresses, including those due to solvent mass uptake and clamping between flow plates, which causes Nafion to creep. Creep can result in membrane thinning and pinhole formation, which increase the incidence of methanol crossover, the leading failure mechanism in DMFC's. Temperature and solvent activity strongly affect the viscoelastic response of Nafion. Thus, an accurate knowledge of the mechanical properties of the membrane under a range of environmental conditions is crucial to improved design and performance of the fuel cell.

The viscoelastic response of Nafion was measured over a range of temperatures and methanol activities in a specially designed apparatus using viscoelastic creep. Additionally, the effect of drying time and temperature on creep results were examined. Finally, membrane swelling dynamics and equilibrium membrane swelling were investigated, as membrane swelling is closely related to creep in fuel cell membranes.

It was found that, in general, increased temperature increases creep by decreasing the bonding strength between polymer strains. However, the combined effects of temperature

and solvent activity are more complicated. It was shown that at room temperature increased methanol activity causes greater creep. This increase is due to the increased free volume which occurs with the addition of methanol, and thus increased mobility of side chains, which causes more creep to occur. At intermediate temperatures 50 and 60 °C, a local maximum in creep was seen at a very low methanol activity. These results are similar to those found by Majsztrik for Nafion creep in water, in which a local maximum at intermediate activities was found for these temperatures. In methanol, the position of the local maximum with activity has simply shifted. These results were explained by solute induced changes of the microphase separation in Nafion. As temperature and solute activity change, the hydrophilic microphase restructures itself. Less creep occurs in phases in which the hydrophilic and hydrophobic phases are more separated.

Nafion's mechanical properties were also shown to be strongly dependent on thermal history. Drying temperature affects creep by causing rearrangements in the microstructure of Nafion which may or may not return to its original state upon cooling. The results of the drying process are a mix of thermodynamics and kinetics, and are thus also dependent on drying time.

The final morphology of Nafion is a function of thermal history, temperature, solvent type, and solvent activity. It was found that all of these factors have a significant effect on the viscoelastic response of Nafion®. Results were explained based on changes in microstructure and interactions within Nafion®.

# Acknowledgements

I would like to begin by thanking my advisor, Professor Jay Benziger, for all of his help and support throughout the writing of this thesis. Professor Benziger gave me a lot of freedom to work under my own direction while also offering generous help when it was needed. He was always incredibly quick to respond to emails and provide input on my work. I also gratefully acknowledge the financial support and use of lab space I received from Professor Benziger.

I would also like to acknowledge all the members of the Benziger lab group. It was a pleasure to get to know and work with Erin, May Jean, Josh, Makini, and Ellazar, as well as to work alongside fellow seniors Roxy, Hannah, and Taylor. Thanks for letting me into lab when I was locked out, helping me with Labview, and putting up with me turning off the lights when I left the room when they were in there working.

Perhaps the most important acknowledgement is to Paul Majsztrik, without whom this thesis would not be possible. Paul's dissertation was an invaluable source for this thesis, providing both motivation for my topic and explanation for some of my results. Paul also provided the initial instruction and direction for my experimental work. He was always there when I had questions, with quick and helpful responses to my emails and even phone calls. I have been honored to have Paul as a teacher, lab buddy, and friend.

I would like to thank my family and friends for their support throughout the year. A big hug and thank you to Duane, Harriet, Pet, and Baby Tigger for always being there and making my year so happy-fantastic so far. Shout out to the Hurricane Gang for how much fun they are going to make senior spring once this thesis is finished, especially the roomies Mark, Jake, Katie, Molly J., Will, Evan, and Molly R, honorary roommate and great friend. Finally, I would like to thank Mom, Dad, Katie, and Barclay, for their love and support, which I appreciate so much, no matter how far away you may be.

# Table of Contents

Abstract.....	ii
Acknowledgements .....	iv
Table of Contents.....	v
Table of Figures.....	vii
1. Introduction .....	1
1.1 Motivation for Fuel Cells.....	1
1.2 Direct Methanol Fuel Cells.....	2
1.2.1 Introduction and Operating Principles.....	2
1.2.2 Fuel Cell Components .....	3
1.2.3 Advantages and Disadvantages of the DMFC .....	4
1.2.4 Role of the membrane in the fuel cell .....	6
1.3 Nafion® .....	6
1.3.1 Introduction .....	7
1.3.2 Morphology.....	8
1.4 Importance of Mechanical Properties .....	9
1.4.1 Introduction .....	9
1.4.2 Temperature and Humidity Effects on Mechanical Properties .....	9
1.5 Thesis Overview .....	10
2. Background- Effects of Temperature and Solvent Activity on Tensile Creep in Nafion .....	11
2.1 Introduction .....	11
2.2 Microstructure of Nafion .....	12
2.3 Tensile Creep.....	14
2.3.1 Significance in Fuel Cells .....	14
2.3.2 Principles of Creep .....	15
2.4 Temperature and Solvent Effects .....	16
2.4.1 Temperature Effects .....	16
2.4.2 Solvent Activity Effects.....	17
2.5 Membrane Swelling .....	17
2.6 Thermal History Effects.....	18
2.7 Solvent Type.....	18

3. Experimental Procedure .....	20
3.1 Tensile Creep Apparatus .....	20
3.2 Experimental Procedure .....	23
3.2.1 Preparation of Materials .....	23
3.2.2 Tensile creep testing .....	23
3.2.3 Thermal History Effects .....	25
3.2.4 Solvent Effects .....	26
4. Experimental Results and Discussion .....	27
4.1 Introduction .....	27
4.2 Membrane Swelling .....	27
4.2.1 Swelling Dynamics .....	27
4.2.2 Equilibrium Swelling Strain .....	28
4.3 Nafion® Creep Response in 100% Methanol .....	30
4.3.1 Introduction .....	30
4.3.2 Results .....	30
4.3.3 Discussion .....	38
4.5 Thermal History Effects .....	45
4.5.1 Results .....	45
4.5.2 Discussion .....	49
4.5 Solvent Effects .....	50
5. Conclusion .....	56
References .....	60

# Table of Figures

Figure 1.1 Schematic of a Direct Methanol Fuel Cell (not to scale) (Liu 2002).....	5
Figure 1.2 Structural formula of Nafion (Elliot, 2000).....	8
Figure 2.1 Phase diagram for microphase separation in block copolymers (Benziger, 2008).....	14
Figure 2.2 Plot of ideal creep response.....	17
Figure 3.1 Schematic of Majsztrik's creep instrument with environmental control (Majsztrik, 2007).....	23
Table 3.1 Cleaning procedure for Nafion® .....	24
Figure 3.2 Length of Nafion® during drying procedure (Majsztrik, 2007).....	25
Table 3.2 Outline of experimental procedure for tensile creep testing.....	26
Figure 4.1. Membrane swelling dynamics for Nafion at 23°C at different methanol activities....	29
Figure 4.2 Membrane Swelling after 12 hours equilibration at different methanol activities....	30
Figure 4.3a Nafion® creep response for different methanol activities at 23°C.....	32
Figure 4.3b Nafion® creep recovery for different methanol activities at 23°C.....	32
Figure 4.3c Creep strain and components at 23°C as a function of water activity.....	33
Figure 4.4a Nafion® creep response for different methanol activities at 50 °C.....	34
Figure 4.4a Nafion® creep recovery for different methanol activities at 50 °C.....	34
Figure 4.5a Nafion® creep response for different methanol activities at 60 °C.....	35
Figure 4.5b Nafion® creep recovery for different methanol activities at 60 °C.....	35
Figure 4.4c Creep strain components at 50°C as a function of water activity.....	36
Figure 4.5c Creep strain components at 60°C as a function of water activity.....	36
Figure 4.6 Plot of creep strain components at 23°C as a function of methanol activity.....	37
Figure 4.7 Plot of creep strain components at 50°C as a function of methanol activity.....	37
Figure 4.8a-f Creep strain components vs. temperature for different activities.....	38
Figure 4.9 Nafion creep response for different water activities and temperatures (Majsztrik, 2007).....	42
Figure 4.10 Phase diagram for microphase separation in block copolymers (Benziger, 2008).....	44
Figure 4.11 Creep strain components at 23°C as a function of methanol activity for different drying conditions.....	47
Figure 4.12a Nafion creep response at 23 °C for different activities and drying temperatures (dried for 3 hours).....	48



Figure 4.12b Nafion creep recovery at 23 °C for different activities and drying temperatures (dried for 3 hours).....	48
Figure 4.13a Nafion creep response at 23 °C for different activities and drying temperatures (dried for 12 hours).....	49
Figure 4.13b Nafion creep recovery at 23 °C for different activities and drying temperatures (dried for 12 hours).....	49
Figure 4.14 Comparison of total creep strain for the three solvent types.....	52
Figure 4.15a Nafion creep response at 23 °C for 50/50 methanol/water mixtures (by mol fraction).....	53
Figure 4.15b Nafion creep recovery at 23 °C for 50/50 methanol/water mixtures (by mol fraction).....	53
Figure 4.16a Nafion creep response at 60°C for 50/50 methanol/water mixtures (by mol fraction).....	54
Figure 4.16b Nafion creep recovery at 60°C for 50/50 methanol/water mixtures (by mol fraction).....	54
Figure 4.17. Nafion® creep response at 23°C for various water activities. (Courtesy of Majsztrik).....	56
Figure 4.18. Nafion® creep response at 50°C for various water activities. (Courtesy of Majsztrik).....	56

# 1. Introduction

## 1.1 Motivation for Fuel Cells

As fossil fuel reserves are depleted and global warming becomes a larger concern, alternative technologies for providing clean energy to the world are receiving increasing attention. The Polymer Electrolyte Membrane (PEM) fuel cell will very likely play an important role in building a renewable energy economy. PEM fuel cell applications range from power sources for vehicles to cell phone batteries to energy storage applications. Fuel cells are receiving increasing attention due to significant technical advances. However, in order for the fuel cell to become commercially competitive, further developments in technology are needed.

A fuel cell is an electrochemical device which converts chemical energy from a variety of fuels into electrical energy. The most common type, the hydrogen fuel cell, is based on the electrochemical reaction of hydrogen and oxygen. However, in recent years, direct methanol fuel cells (DMFCs) have received increasing attention, especially as power sources for various portable devices. Electronic devices today are smaller than ever, but the size of the batteries is a roadblock to further miniaturization. DMFC's are an ideal solution to this problem because they can store very high energy content in a small space. Direct methanol fuel cells are still a relatively new technology, but as they are put to more uses and become better understood, applications may spread to other sectors, such as transportation and energy storage.

Fuel cells are still expensive compared to the traditional fossil fuel sources. In order for fuel cells to become more practical for everyday commercial use, many technical challenges must be overcome. Durability, reliability, and performance must increase while price and weight decrease (Majsztrik, 2007). In order to address some of these challenges, this thesis will focus on the membrane material, an integral part of PEM fuel cells. It will investigate the mechanical properties of the most common polymer electrolyte membrane, Nafion<sup>®</sup>, at a range of temperatures and solvent activities.

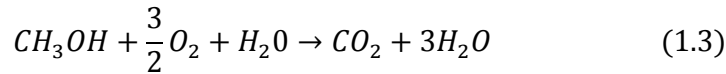
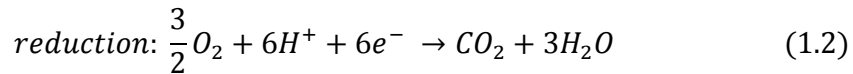
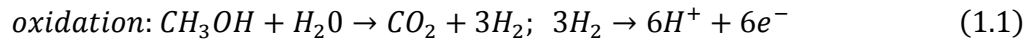
## **1.2 Direct Methanol Fuel Cells**

### *1.2.1 Introduction and Operating Principles*

A fuel cell is an electrochemical energy conversion device which converts the chemical energy from a variety of fuels into useful electrical energy. Perhaps the most important property of a fuel cell is that unlike those of a battery, reactants and products of a fuel cell are continuously fed to and removed. There are many types of fuel cells, including Proton Exchange Membrane (PEM), Solid Oxide, Alkaline, Molten Carbonate, and Direct Methanol Fuel Cells (DMFC's). Both PEM and Direct Methanol Fuel cells utilize membranes like Nafion<sup>®</sup>; however due to the nature of the solvents used, this thesis will focus mainly on DMFC's.

A DMFC is a type of PEM fuel cell in which the fuel, methanol, is not reformed, but fed directly into the fuel cell. The methanol and water feed is internally reformed on the catalyst layer. The hydrogen is then oxidized at the anode to produce hydrogen ions and electrons. This complex oxidation process is shown in equation 1.1. The electrons travel through the external circuit where they can do useful work. The hydrogen ions travel

through the polymer electrolyte membrane to the cathode and react with oxygen and the electrons from the external circuit to form water, according to equation 1.2. The overall cell reaction is thus the reaction of methanol and oxygen to produce water and carbon dioxide, shown in Equation 1.3.



### 1.2.2 Fuel Cell Components

The DMFC electrode/electrolyte system is a three layer membrane and electrode assembly (MEA). An ionomeric membrane, usually Nafion® is sandwiched between the anode and cathode catalyst layers. Electrodes are usually made with woven carbon cloth or carbon paper. On the side facing the membrane, both the anode and cathode are coated with a porous platinum-based catalyst. There are normally highly porous conductive carbon fabric gas diffusion layers (GDLs) between the catalyst layer and the electrode. The GDLs collect current from the catalyst layers and inhibit mass transport of reactants and products between the electrodes and the flow fields (Liu, 2002). A good three-phase contact between the membrane, the porous electrodes, and the gas is very important for performance. The MEA is clamped between a pair of graphite blocks which are electrically conducting and contact the electrodes. They contain flow channels which distribute the reactants and products to the anode and cathode. A schematic of a typical DMFC is shown in Figure 1.1.

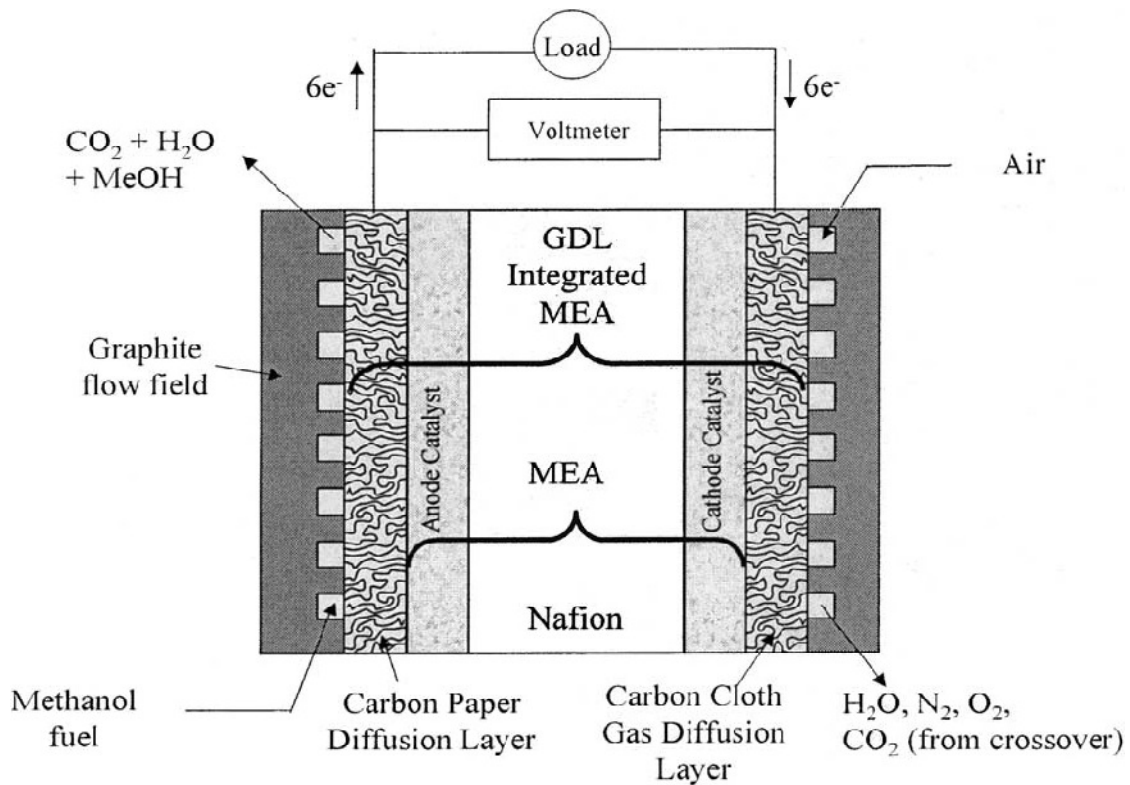


**Figure 1.1 Schematic of a Direct Methanol Fuel Cell (not to scale) (Liu 2002)**

### *1.2.3 Advantages and Disadvantages of the DMFC*

The DMFC has several important advantages over the conventional hydrogen fuel cell. First of all, the fuel, liquid methanol, does not need to be externally reformed, but is fed directly into the fuel cell. The system produces electric power by direct conversion of methanol at the anode. Therefore, complicated and expensive catalytic reforming of the fuel is not needed. This is particularly attractive for transportation applications, which rely on bulky and often unresponsive reformer systems to convert methanol or other hydrocarbon fuels to hydrogen (Hogarth, 1996). Also, methanol storage is much more convenient than hydrogen storage because it does not need to be at high pressures or low temperatures. Methanol is a liquid from -97 to 64.7 degrees Celsius at a pressure of 1 bar

(Lamy et.al, 2002). Another main advantage of the DMFC is that it can store high energy content in a small space. The energy density of methanol is an order of magnitude greater than highly compressed hydrogen and 20-30 times that of lithium-ion, the primary storage component of the best batteries (Holladay, 2002). This makes the DMFC ideal for small portable devices such as laptops and cell phones. However, despite high their high energy density, the power density of DMFC's is still significantly lower than their hydrogen counterparts. Power densities of up to  $0.3 \text{ W/cm}^2$  have been obtained for small PEM hydrogen fuel cells (Scholta, 2006), whereas the maximum power density for small DMFC's is about  $50 \text{ mW/cm}^2$  (Chang, 2002).

Despite these advantages, commercialization of the DMFC has been impeded due to its poor performance compared with hydrogen fuel cells. Low-temperature reformation of methanol to hydrogen and carbon dioxide requires a highly efficient catalyst. Studies have shown that only expensive platinum-based materials show reasonable activity and the required stability (Hogarth, 1996), and the DMFC requires a larger quantity of this platinum catalyst than conventional PEMFC's. A key problem with DMFC's is the high permeation of methanol through the membrane from the anode to the cathode, a process known as methanol crossover. This results in lower efficiency and sluggish dynamic behavior. Furthermore, a DMFC can only produce limited power, and the output power of the cell is dependent on temperature and the quantity of fuel in the fuel cell. Recent work by Majsztrik and Satterfield has shown that the mechanical and transport properties of Nafion® are affected by water. A similar effect on mechanical properties may occur with methanol, and this will affect the occurrence of methanol crossover.

PEM electrolyte materials have extended the operation temperature of the DMFC beyond those attainable with traditional liquid electrolytes, which has lead to major improvements in performance in recent years. However, reliability, performance and cost need to improve before the implementation of the DMFC can become widespread.

#### *1.2.4 Role of the membrane in the fuel cell*

The membrane is a central component of the PEM fuel cell. The purpose of the membrane is to physically separate the fuel from the oxidant, while allowing protons to move across the membrane but not electrons. Thus, it must transport protons with little resistance and be a poor conductor of electrons. When the Nafion® is dry, its acid groups are tightly bound, like a salt, and don't allow any proton conduction. A solvent such as water or methanol is essential for proton conductivity. For example, water has been found to increase membrane conductivity by several orders of magnitude going from dry to fully saturated (Yang, et. al., 2004).

The material must also be mechanically and chemically stable under the range of operating conditions of the fuel cell environment, such as temperature, pressure, and solvent activity. This means that its properties should not change too much under different conditions. There are very few materials that do this well. Nafion, the most commonly used membrane in PEM and Direct Methanol Fuel Cells, doesn't accomplish all of these criteria well, but it is the only ionomer with a lifetime greater than 1000 hours in a fuel cell environment. Therefore, further research is needed to determine how the properties of Nafion® as a fuel cell membrane can be improved.

### **1.3 Nafion®**

### 1.3.1 Introduction

The membrane studied in this work is Nafion<sup>®</sup>, which is a sulfonated tetrafluoroethylene copolymer, the first of a class called perfluorinated ionomers. It was developed by DuPont in the late 1960's for use in the chlor-alkali process. Since then, Nafion<sup>®</sup> has become the most commonly used PEM fuel cell membrane material due to favorable conductivity, chemical and mechanical stability, and mechanical toughness. The molecular structure of Nafion<sup>®</sup> is shown below. The value of  $m$  is usually one, so that the value of  $n$  determines the ratio of polar to non-polar material in the compound.

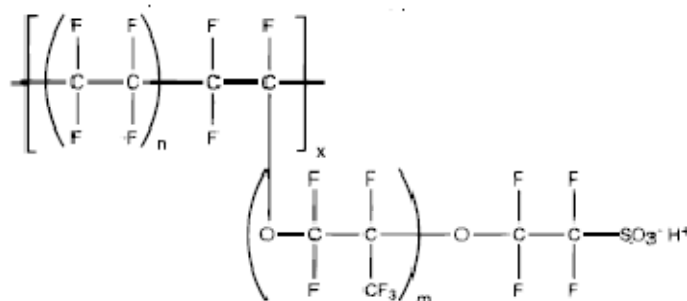


**Figure 1.2 Structural formula of Nafion (Elliot, 2000)**

The structure of Nafion<sup>®</sup> is shown in Figure 1.2. Nafion<sup>®</sup> consists of a fluorinated-carbon backbone with perfluoroether (PFE) side chains ending in sulfonic acid groups (Elliot, 2000). The backbone is tetrafluoroethylene (TFE) or Teflon-PTFE<sup>®</sup>, and gives Nafion<sup>®</sup> its strength and toughness. The sulfonic acid side groups are arranged at intervals along the backbone. These give Nafion<sup>®</sup> its chemical and mechanical stability. Conventionally, membranes are named according to their equivalent weight (EW) and thickness. For example, Nafion<sup>®</sup> 1110, which is used in our lab, has an EW of 1100 g/mol-SO<sub>3</sub> and a thickness of 0.010".



### *1.3.2 Morphology*

The detailed characterization of Nafion is important for the development of all its technical applications. Although Nafion's® morphology has been the subject of extensive research since the 1970's, the exact structure of Nafion® is still not known. Several models have been proposed which were summarized by Roberson, including the Eisenberg Model of Hydrocarbon Ionomers, the Gierke Cluster Network Model, the Mauritz-Hopfner Model, and the Yeager Three Phase Model (Robertson, 1994). The most widely adopted model is the one first proposed by Gierke, which assumes that the hydrophilic groups aggregate into clusters which grow in size with increasing hydration (Benziger, 2008).

All models agree on the fact that that Nafion® phase separates into discrete hydrophobic and hydrophilic regions. The hydrophobic region is the fluorocarbon backbone, and the hydrophilic region is the PFE side chains terminating in sulfonic acid groups. Small angle X-ray scattering (SAXS) and neutron scattering experiments have clearly shown that ionic clustering is present in Nafion®, in which the ionic groups tend to form tightly packed regions called clusters as a result of electrostatic interactions (Yeager et. al, 1982). However, the details of the arrangement of the clusters are not known exactly.

The information on the structure of Nafion® depending on water content was summarized nicely in the recent work of Mauritz and Moore (Mauritz, 2004): The morphology of the Nafion® reorganizes as the dry membrane is swollen with water. The dry state consists of isolated spherical ionic clusters with diameters of around 1.5 nm dispersed in the perfluorinated matrix. When the ionomer takes up water, the clusters start to hydrate and their diameters increase up to 4 nm. They form "nano-pools" of water that are

surrounded by ionic sulfate groups that are connected by tiny channels. Very little work has been done regarding Nafion's® structure with methanol uptake.

## **1.4 Importance of Mechanical Properties**

### *1.4.1 Introduction*

Studies of polymer electrolyte membrane (PEM) fuel cell dynamics using Nafion® membranes have demonstrated the importance of membrane mechanical properties to performance and longevity of the cell (Satterfield 2007). Thus, an understanding of the mechanical properties of membranes in PEM fuel cells is essential to improving the efficiency, performance, and cost of the fuel cell. One of the most important mechanical properties studied in fuel cell membranes is tensile creep. In a Direct Methanol Fuel Cell, creep results in mechanical problems that increase the incidence of methanol crossover, the leading failure mechanism in DMFC's. Additionally, a material's mechanical properties are strongly dependent on the temperature and solvent activity of their environment.

### *1.4.2 Temperature and Humidity Effects on Mechanical Properties*

One of the main faults of Nafion® as a fuel cell membrane material is that its mechanical properties are strongly dependent on temperature and hydration. Due to the nature of the reactants and products, fuel cells operate at elevated humidities (or solvent activities). Furthermore, increasing the operating temperature of fuel cells is desirable for several reasons. However, common fuel cell membranes including Nafion® perform poorly under these conditions and degrade more quickly. Improving membrane performance over a variety of conditions simplifies operation controls and improves overall performance.

Because of this, an understanding of the mechanical properties under a range of conditions is very important, although very little work has been done in this area.

## **1.5 Thesis Overview**

This thesis will present studies on the mechanical properties of Nafion<sup>®</sup>, specifically with respect to viscoelastic creep and membrane swelling. It will investigate the effects of both methanol and water on the viscoelastic response of Nafion<sup>®</sup> membranes. As fuel cells are operated at elevated temperatures and humidity, it is important to take environmental conditions into account when studying membrane mechanical properties. Thus, effects due to methanol in the presence and absence of water will be studied at different temperatures and solvent activities. A unique apparatus built by Paul Majsztrik of Princeton University allows for an analysis of viscoelastic response at carefully controlled temperature and humidity, an area in which very little work has been possible in the past due to limitations in experimental equipment. Additionally, the effect of drying time and temperature on creep results will be examined. Finally, membrane swelling dynamics and equilibrium membrane swelling will be investigated, as membrane swelling is closely related to creep in fuel cell membranes. The primary goal of these experiments is to gain a better understanding of Nafion's morphology, a subject that is still debated in the field despite extensive studies performed on the polymer. Thus, experimental results will be attempted to be explained based on microstructure and interactions at a molecular level. A secondary goal is to determine pretreatment and environmental conditions for Nafion that maximize its mechanical performance.

## **2. Background- Effects of Temperature and Solvent Activity on Tensile Creep in Nafion**

### **2.1 Introduction**

Nafion® is a viscoelastic material, which means that it responds to stress in a time-dependent manner. The membrane of a PEM fuel cell is subject to various stresses, for example, strain from changing levels of hydration as the membrane takes up water and swells. The clamping of the membrane between flow plates also puts stress on the membrane. These stresses will cause a membrane such as Nafion® to flow and respond dynamically to changes in hydration and stress. An accurate knowledge of the mechanical properties of the membrane is crucial to increased understanding of its failure mechanisms and therefore can lead to improved design and performance of the fuel cell. One of the most commonly studied mechanical properties and the main subject of this thesis is tensile creep. Creep is the term used to describe the time dependent deformation of a material in order to relieve applied stresses.

The mechanical properties of Nafion have been the subject of extensive studies since the polymer's development in the 1960's. However, due to constraints in available equipment, few studies have been done on the mechanical properties of Nafion under a wide range of temperatures and humidities. Majsztrik's creep apparatus with environmental control has resulted in extensive studies of Nafion's® viscoelastic response over a range of temperatures and water activities (Majsztrik, 2007). To the author's knowledge, no such studies have been done using methanol. The goal of this thesis is to present results related to the viscoelastic response of Nafion over a range of temperatures and methanol activities. The major areas of study are as follows:

- 1) Equilibrium Membrane Swelling
- 2) Effects of solvent activity and temperature on creep response
- 3) Thermal history effects
- 4) Solvent effects

## **2.2 Microstructure of Nafion**

Dependence of mechanical properties of Nafion on both temperature and solvent activity suggest that there are structural changes in Nafion which result in changes in mechanical properties. Therefore, an understanding of the microstructure of Nafion is extremely important for predicting the effect of the environmental conditions on mechanical properties of Nafion®.

Microphase separation in block copolymers is a well-known phenomenon, however, it has been suggested that phase separation also occurs with random copolymers, such as Nafion® (Benziger, 2008). The basic principle behind microphase separation is that phases restructure themselves so as to minimize free energy. In Nafion®, different phases form to try to minimize the interaction between the hydrophobic and hydrophilic phases. Nafion has the unique property that its two components exhibit very different hydrophilicities. The TFE backbone is very hydrophobic while the strong hydrogen bonding capacity of the sulfonic acid groups makes them very hydrophilic.

It is possible to continuously vary the volume fraction of the hydrophilic phase by controlling the activity of a hydrogen bonding solute surrounding the polymer (Benziger, 2008). It has been proposed that a change in the volume fraction of the hydrophilic vs. the hydrophobic phase due to absorbed solute results in microphase evolution from dispersed, to cluster, to cylindrical phases with increasing solute activity (Benziger, 2008). This

microphase evolution also depends on temperature; an increase in temperature decreases the interaction parameter, generally the Flory parameter  $\chi$ . It is the combined effects of temperature and solute activity which lead to a restructuring of the hydrophilic microphase, thus a change in mechanical properties. Thus, microphase separation is a function of the volume fraction of the hydrophilic phase  $\phi$ , the energy difference between monomers  $\chi$ , and thus the temperature  $T$ . Figure 2.1 is a phase diagram developed for block-copolymers developed by Matsen and Bates (1996) and modified by Benziger (2008). Since Nafion is a random copolymer, we do not expect phase transitions to be exactly the same as block copolymers, but we do know that the driving forces for microphase separations should be very similar, and thus we expect similar qualitative behavior.

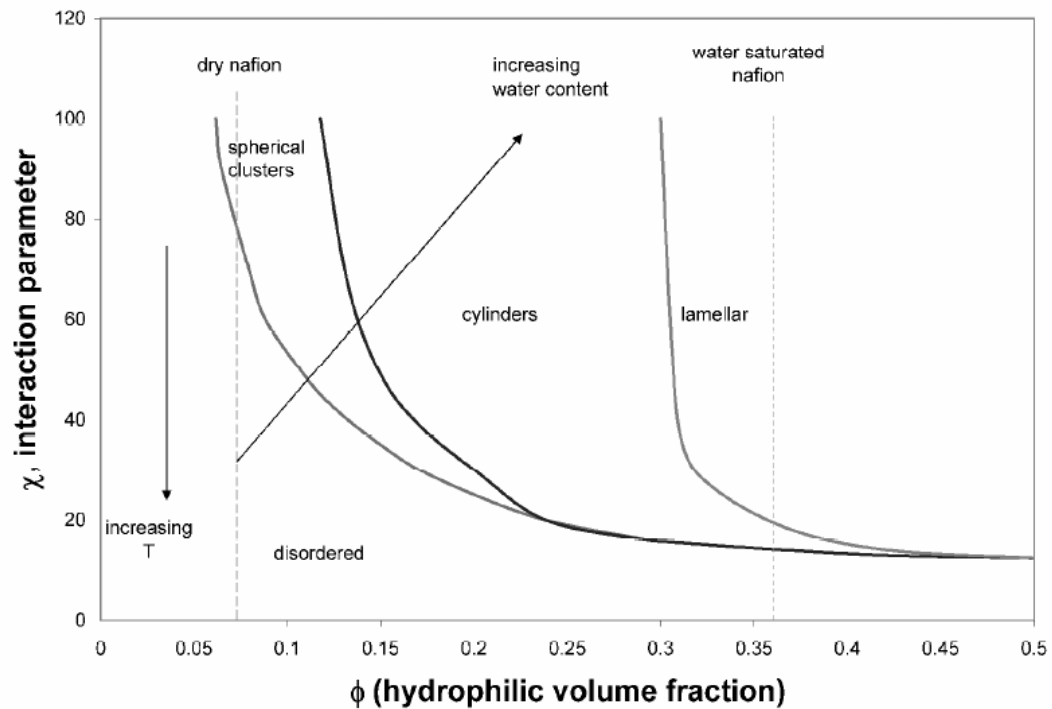


Figure 2.1 Phase diagram for microphase separation in block copolymers (Benziger, 2008)

## 2.3 Tensile Creep

### 2.3.1 Significance in Fuel Cells

In a fuel cell membrane, creep can result in membrane thinning, the formation of pinholes, and the development of contact problems between the membrane and the electrode, all of which can lead to the failure of the PEM fuel cell (Majsztrik, 2007). Pinhole formation is an especially large problem for DMFC's because it increases the occurrence of methanol crossover, the leading failure mode DMFC's. In addition, creep increases the area methanol permeation, which causes more methanol crossover to occur. Methanol crossover is a process by which methanol moves from the anode to the cathode through the membrane. It leads to power loss due to i) oxidation of methanol at the cathode, causing unwanted consumption of oxygen, ii) poisoning of the cathode by CO, an intermediate product of methanol oxidation, and iii) excessive water buildup by the cathode produced by methanol oxidation (Lin et. al., 2006) Methanol crossover not only lowers fuel utilization efficiency, but also further increases the size and complexity of the fuel cells in order to manage the excess heat and water produced as methanol is oxidized on the air side of the fuel cell (Jiang, 2004). Therefore, if creep strain in Nafion could be reduced by varying pretreatment or environmental conditions, fuel cell performance could be improved.

Reliability of PEM fuel cell power systems is mostly dependent of the durability of the Membrane Electrode Assembly (MEA). Thus, it is extremely important to understand the mechanical properties of the Nafion® membrane, as it leads to increased understanding of failure mechanisms of the Membrane Electrode Assembly. Furthermore, accurately knowing the mechanical properties of Nafion® at a range of temperatures and solvent activities leads to better modeling of fuel cell performance under many different possible

environmental conditions. In addition, the dynamics of fuel cell power response are partially dependent on mechanical properties (Satterfield et. al., 2006).

### 2.3.2 Principles of Creep

Creep is the term used to describe the time dependent deformation of a material in order to relieve applied stresses. It is an excellent technique for characterizing the viscoelastic response of a material. Creep is measured simply by applying a constant stress  $\sigma$  to the material and recording the resulting strain  $\epsilon$  which increases with time. Stress and strain are defined by the following equations:

$$\text{Stress: } \sigma = F/A$$

$$\text{Strain: } \epsilon = \frac{\lambda - \lambda_0}{\lambda_0}$$

where  $F$  is the applied force,  $A$  is the cross sectional area of the material, and  $\lambda_0$  and  $\lambda$  are the initial and final lengths of the material, respectively.

There are three components of an ideal creep response. Instantaneous elastic creep ( $\epsilon_e$ ), occurs immediately and is completely recoverable. This is simply due to the stretching and bending of bonds between chains. Following this, strain increases with time at a decreasing rate in the delayed elastic ( $\epsilon_d$ ) creep phase. This component is also completely recoverable, and is the result of these chains uncoiling. Finally, viscous flow ( $\epsilon_v$ ) occurs due to chain slipping, which is irrecoverable. The contribution of these different components can be separated by allowing a sample to creep under stress and then undergo recovery under zero stress. The three components of ideal creep response are shown in Figure 2.2.



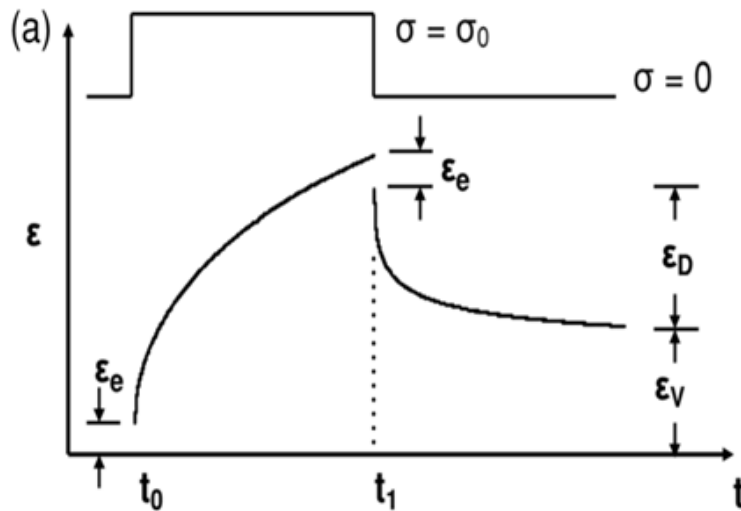


Figure 2.2 Plot of ideal creep response (Majsztrik, 2007)

## 2.4 Temperature and Solvent Effects

### 2.4.1 Temperature Effects

Increasing the operating temperature of fuel cells is desirable because it decreases CO poisoning of the catalyst. CO and H<sub>2</sub> compete to absorb on the platinum based catalyst. Below 100°C, if the concentration in CO is higher than 1-10 ppm, CO will win this competition, which results in a decline in performance. As the temperature of the fuel cell increases, more and more CO can be tolerated. Higher operating temperatures also make the rejection of waste heat easier. However, common fuel cell membranes including Nafion® perform poorly at elevated temperature and degrade more quickly.

As would be expected, the mechanical properties of Nafion® are strongly dependent on temperature, due to the fact that the bonding strength between polymer chains decreases with increasing temperature. As temperature increases, the thermal energy of Nafion's® molecules eventually becomes greater than that of the polymer's secondary bonds, and chains are able to move past one another when a force is applied. Secondary

bonds in Nafion® include hydrogen bond cross-linking between the sulfonic acid groups and Van der Waals interactions between main chains.

#### *2.4.2 Solvent Activity Effects*

Solvent activity, of both methanol and water, strongly affects Nafion's® mechanical properties. Solvent activity is closely related to solvent mass uptake, as increased solvent activity should result in increased uptake. Several studies, including those of Tsai and Hwang (2007) and Majsztrik (2007) have shown that solvent uptake strongly affects the mechanical properties of the polymer. Other studies have shown that solvent uptake results in changes in the size, shape and number of acid clusters of Nafion® (Hsu et. al, 1983). Previous studies have been restricted to measuring properties as a function only of temperature or a very limited range of hydrations. This thesis will investigate solvent activities ranging from 0 to ~1 for both 100% methanol and a 50/50 methanol/water mixtures at different activities. Extensive studies for 0-100% relative humidity have already been performed by Majsztrik (Majsztrik, 2007). Some of the results of these studies will be included in this thesis for comparative purposes.

### **2.5 Membrane Swelling**

Exposing Nafion® to methanol vapor results in uptake of methanol by the polymer, referred to as equilibrium mass uptake. Equilibrium mass uptake is a strong function of the methanol activity, and also depends weakly on temperature. It is what causes Nafion® to swell, among other things. Swelling is very important in the context of fuel cells because since the membrane is clamped between two plates, swelling due to mass uptake causes stresses in the membrane, which result in strain. This swelling strain is a

result of polymer reorganization as methanol content changes. Equilibrium mass uptake is also important in fuel cells because proton conductivity is dependent on solvent activity (Duplessix et. al, 1979).

## **2.6 Thermal History Effects**

Studies have shown that Nafion's® performance and intrinsic properties are dependent not only on its chemical identity but also on its thermal history, for example, drying and exposure to high temperature (Hensley et.al., 2007). Therefore, when using Nafion® for fuel cells or any application, one must take careful account of thermal history. Ideally, a pretreatment procedure would be developed for Nafion® that would result in optimal performance of the membrane. Drying is an important part of pretreatment, and can have a significant effect on Nafion's® mechanical properties. Temperature changes may cause a change in morphology, which would change the creep response of the polymer. Changes in morphology may also be dependent on the amount of time exposed to drying conditions.

## **2.7 Solvent Type**

There are two relevant solvents in a DMFC: methanol and water. Since methanol is fed directly into the cell as fuel, clearly the membrane will be exposed to methanol. The reaction at the cathode produces water (see equation 1.1), but water is also required at the anode side of the DMFC in order to maintain the reaction. Conventional DMFC systems have an active water management system with a water recovery pump and a recirculation pump to achieve this. Thus, the membrane is exposed to both methanol and water during fuel cell

operation. Nafion's® ionic groups can absorb water and methanol, which alters the bonding between polymer chains and therefore also the mechanical properties (Majsztrik, 2007).

Solvents that were a mixture of methanol and water were investigated to determine the synergistic effects of methanol and water on Nafion® creep response, as well as to compare creep response when the membrane is exposed to water, methanol, or a combination thereof. This allows one to gain a further understanding of the solvent interactions with Nafion® that give rise to its mechanical properties. Clearly, the solvent type will affect creep response due to differing interactions between different solvents and the Nafion®, as well as possible differences in mass uptake of the two solvents by Nafion®.

## 3. Experimental Procedure

### 3.1 Tensile Creep Apparatus

Commercially available instruments for testing mechanical properties of materials offer little control over solvent activity over a range of temperatures. The apparatus (patent pending) used in this experiment was designed by Paul Majsztrik of Princeton University specifically to measure creep response of Nafion® under a controlled environment of temperature and water activity. It was a simply matter to modify the experimental procedure already developed by Majsztrik in order to incorporate controlled methanol activity. Figure 3.1 is a schematic of the creep instrument with environmental control.

The environmental creep apparatus is described in detail elsewhere (Majsztrik, 2007), but will be explained briefly here. The sample is clamped between a stationary upper clamp and a moveable lower clamp. A hanging 150.4 gram weight is used to apply uniaxial stress to the sample through a rod connected to the bottom clamp. The clamps allow for a maximum strain of 2.25 for a typical 1" sample. Strain is measured with a Linear Variable Displacement Transducer (LVDT) (Macro Sensors, HSAR 750-2000) by monitoring the position of one section of the rod connecting the hanging mass. This provides a measurement of strain without contact. A universal joint prevents the transmission of torque due to misalignment, while PTFE guides prevent the rod from swinging. The different components of the instruments are mounted on a vertical aluminum plate with leveling feet. A sliding stage is used to apply and relieve the mass from the sample.

An environmental chamber consisting of an insulated outer shell and a humidified inner chamber surrounds the sample. Both chambers sit on a stationary base which also

serves as a mount for sensors and other components needed to control the temperature and solvent activity of the environment. The insulated outer shell consists of this base and a removable upper box insulated with a fiberglass insulation board. The humidity chamber is a Pyrex reaction vessel which sits on a stainless steel base and surrounds the sample.

An isothermal environment is created around the humidity chamber using a finned heater and a fan together with a PID temperature controller. A temperature range of 25 - 250°C is possible. The apparatus also allows for careful control of solvent activity. The activity of a component of an ideal gas mixture is defined as the partial pressure of that component divided by the vapor pressure of the component at the given conditions. However, due to limitations in the experimental apparatus, these partial pressures cannot be directly measured. Therefore, activity is controlled by using mass flow controllers to vary the flow rates of a dry nitrogen stream and a nitrogen stream which passes through the bubbler to become saturated with methanol. Methanol activity is then calculated as the flow rate of the nitrogen stream saturated with methanol divided by the flow rate of the saturated and the dry stream. This calculation is given in equation 3.1. The key assumption made is that the nitrogen stream is completely saturated with methanol. Dry nitrogen gas is used when zero activity is required. The bubbler is contained within the outer environmental chamber to ensure constant gas temperature throughout.

$$\gamma = \frac{Q_{saturated\ N_2} \left[ \frac{mL}{min} \right]}{Q_{dry\ N_2} \left[ \frac{mL}{min} \right] + Q_{saturated\ N_2} \left[ \frac{mL}{min} \right]} \quad (3.1)$$

A Labview program is used to record the length of the sample over time, from which strain can be calculated. Labview provides a straight-forward interface between data

acquisition and the computer. Data is acquired every second for the first 20 minutes of a creep experiment, and once every minute thereafter. Similar data acquisition methods are used for creep recovery.

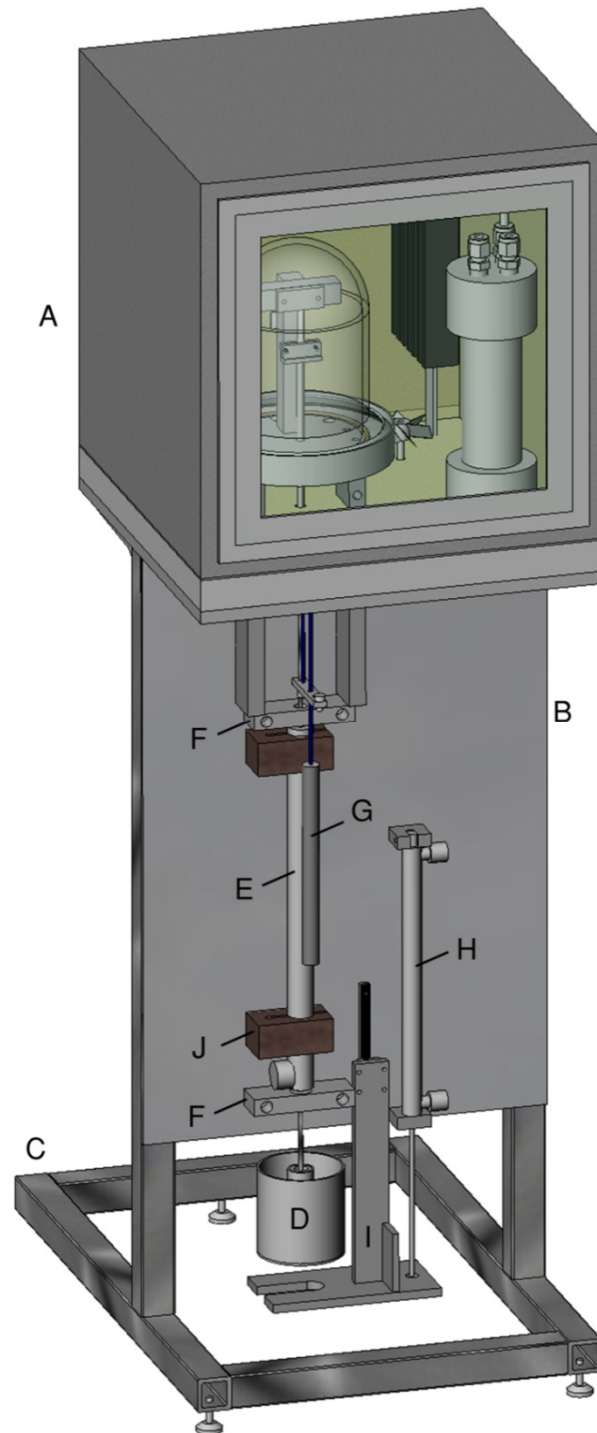


**Figure 3.1 Schematic of Majsztrik's creep instrument with environmental control (Majsztrik, 2007)**

## 3.2 Experimental Procedure

### 3.2.1 Preparation of Materials

All tests were performed on extruded Nafion® N1110 film, which has an equivalent weight of 1,100 g/mol-SO<sub>3</sub> and a dry thickness of 0.0010". Before they can be used in the experiment, extruded Nafion® films must be cleaned and cut. Nafion® films were treated following a standard cleaning procedure developed by Paul Majsztzik, outlined in Table 3.1. After being cleaned, the film is cut into strips of uniform width using a metal template and an Exacto™ knife. The clean Nafion® sample was then mounted in the clamps of the creep instrument using a mounting jig. The jig served to align the sample and hold it in place while it was being clamped.

1. Boil 1 hour in 3% hydrogen peroxide solution
2. Boil 1 hour in distilled/deionized water
3. Boil 1 hour in 0.5 M sulfuric acid
4. Boil 1 hour in deionized water twice.
5. Dry clean polymer flat on lab bench by placing between sheets of filter paper under a relatively heavy weight (Several books, for example) for 48 hours.

**Table 3.1 Cleaning procedure for Nafion®**

### 3.2.2 Tensile creep testing

Tensile creep tests were performed on Nafion® with different methanol activities and over a range of temperatures. Runs were done at 23, 50, and 60°C at activities 0, 0.01, 0.1, 0.35, 0.65, and ~1. In order to compare runs in a meaningful manner, a strict protocol for membrane testing needs to be developed. Sample history (thermal and hydration), applied stress, and sample dimensions are all important factors and must not be varied between runs. The sample must be dried prior to the experiment to remove as much water as possible from the sample. Additionally, the length of time to establish equilibrium



between sample and surroundings must be established. Preliminary experiments were performed in order to determine appropriate times for drying, equilibration, creep, and creep recovery.

Nafion® samples were prepared according the procedure given in Section 3.2.1 and clamped into the creep instrument using a mounting jig. The sample was then dried for at least three hours by running dry nitrogen at 50°C continuously through the chamber. Sample length during drying is plotted in Figure 3.2. The length initially decreases because Nafion® shrinks as it dries. However as Nafion® is heated and dried, its resistance to creep decreases (Majsztrik, 2007). Thus, the increase in length following the initial shrinking is probably due to creep caused by the pressure exerted by the clamping jaws onto the sample. Visual inspection of the samples reveals that they are thinned and widened where clamping occurs.

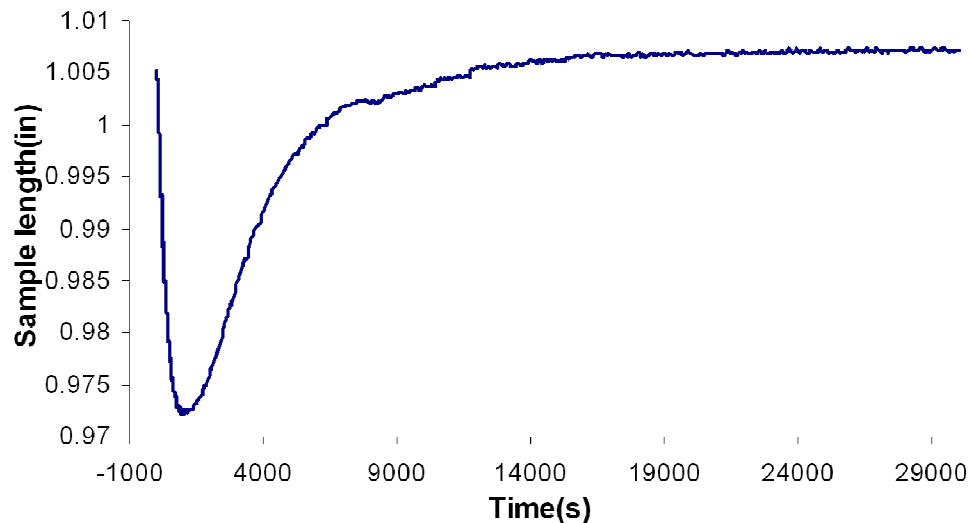


Figure 3.2 Length of Nafion® during drying procedure (Majsztrik, 2007)

After drying, the sample is allowed to reach an equilibrium length while at the desired temperature and methanol activity. The temperature of the environmental chamber was set to the test temperature, and methanol was introduced using the bubbler as described in Section 3.1. Methanol and nitrogen flows are set in order to obtain predetermined methanol activity. It was established that 12 hours was sufficient time for equilibration to occur.

Once equilibrium is established, creep measurements can begin. The sample is subjected to a constant force produced by a suspended weight of 150.4 grams. The sample is allowed to creep for exactly one hour, after which the weight is relieved and creep recovery begins to occur. It was determined that three hours was sufficient time for all creep recovery to occur. During the entire process, sample length was monitored and recorded as a function of time. The overall experimental procedure is outlined in Table 3.2

Step	Flow parameters	Time
Drying	Pure nitrogen at 50°C	3 hours
Heating/cooling (if necessary)	Pure nitrogen at desired temp.	1 hour
Equilibration	Nitrogen/methanol at predetermined activity	12 hours
Creep	Nitrogen/methanol at predetermined activity	1 hour
Creep Recovery	Nitrogen/methanol at predetermined activity	3 hours

**Table 3.2 Outline of experimental procedure for tensile creep testing**

### *3.2.3 Thermal History Effects*

The effects of thermal history on the viscoelastic response of Nafion® were investigated by varying the drying time and temperature from that outlined in the above procedure. Creep runs were carried out at room temperature after drying at both 50 and 100°C for 3 and 12 hours. This was done at three activities: 0, 0.1, and 0.65. Since the boiling

point of methanol is  $64.7^{\circ}\text{C}^{13}$ , the methanol must be removed from the chamber during the drying step at  $100^{\circ}\text{C}$  and reintroduced during the equilibration step.

#### *3.2.4 Solvent Effects*

The synergistic effects of a water-methanol mixture were investigated at  $23^{\circ}\text{C}$ . In addition to a 100% methanol solvent, the experiment was repeated using a solvent of 50% methanol and 50% water. Experiments using 100% water have already been performed by Paul Majsztzik, and were not repeated. However, data from these experiments, courtesy of Majsztzik, is presented in the Results section for comparative purposes. The procedure in Section 2.3.2 for tensile creep testing was followed, with the methanol in the bubbler being replaced with a methanol-water mixture of different compositions. Runs were done at 23 and  $50^{\circ}\text{C}$  for activities 0.01, 0.1, 0.35, 0.65, and  $\sim 1$ .

## 4. Experimental Results and Discussion

### 4.1 Introduction

Creep and creep recovery were measured at over a range of temperatures for various methanol activities. Solvents of both 100% methanol and a 50/50 methanol-water mixture were investigated. Summary data from 100% water, courtesy of Paul Majsztrik, is also presented here for comparative purposes. The effect of thermal history on creep and creep recovery was also investigated. The results from the various studies are presented in this section divided by experimental technique.

### 4.2 Membrane Swelling

#### 4.2.1 Swelling Dynamics

Sample strain was monitored throughout the 12 hour equilibration period in order to gain a better understanding of the swelling dynamics of Nafion® in methanol. The plot in Figure 4.1 shows sample strain over time as the dry sample is exposed to methanol vapor at activities .01, .10, .35, .65, and ~1 at 23°C. As expected, equilibrium swelling strain increases monotonically with methanol activity. The next thing we notice is the effects of the methanol vapor are felt much later in the environmental chamber for lower activities. It takes over 14,000 seconds for the strain at activity .01 to start to increase from zero, whereas for activity .35, it takes only a few hundred seconds. This is probably due to the slow diffusion of methanol through the polymer at low concentration gradients. The initial slope for activity .01 is significantly less than the slopes at higher activities. This means that time for swelling strain to reach its equilibrium value increases significantly at very low activities. The initial slopes for the higher activities are very similar. This is probably due to

interfacial mass transport resistance being the limiting step to water uptake (Majzstrik, 2007). This is based on Satterfield's finding that mass transport limits mass uptake for dry Nafion<sup>®</sup> exposed to water vapor with activity approaching 1.0 (Satterfield, 2007). It is reasonable to infer that one might see a similar result with methanol.

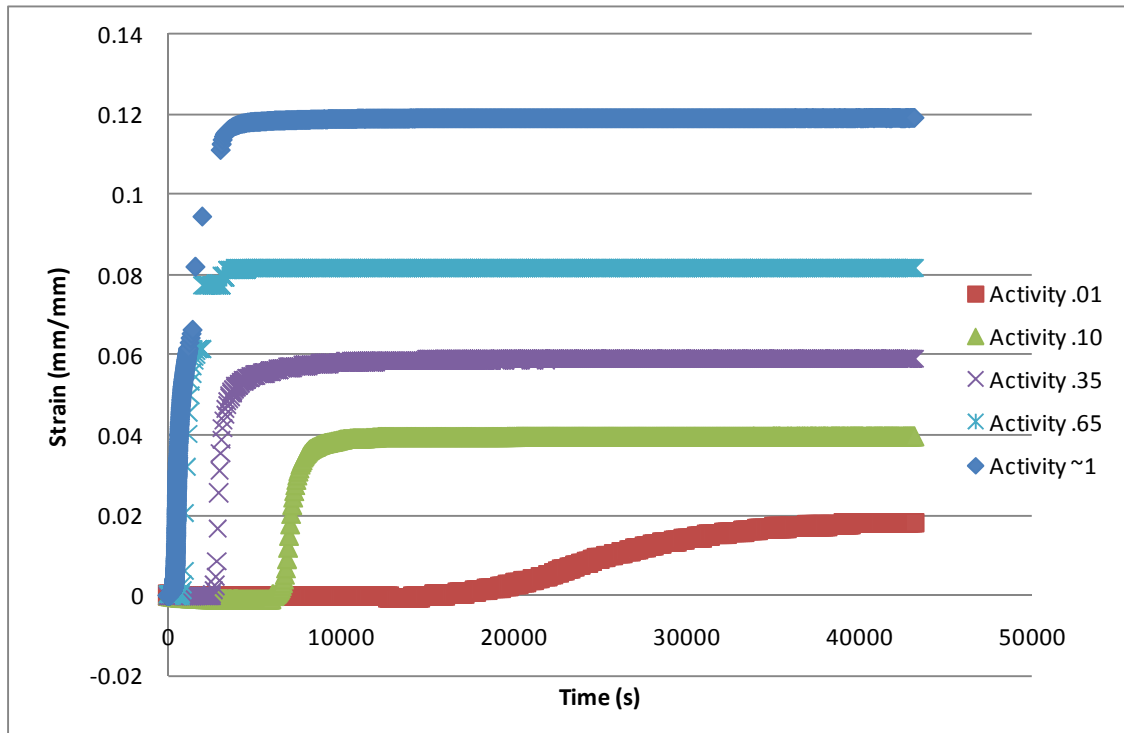


**Figure 4.1. Membrane swelling dynamics for Nafion at 23°C at different methanol activities**

#### 4.2.2 Equilibrium Swelling Strain

Membrane swelling in equilibrium with different solvents was investigated in order to determine the behavior of Nafion<sup>®</sup> in various methanol activities in the absence of any outside stress. This was done for all creep tests performed in this thesis by recording the length of the sample before and after the 12 hour equilibration period and calculating the percentage change in length. The results for methanol at 23, 50 and 60 °C are given in Figure 4.2. As expected, equilibrium swelling increases monotonically with methanol

activity. Little dependence was seen on temperature, which is consistent with the results of Majsztrik for equilibrium swelling in water. It is interesting that samples equilibrating at 60°C consistently seemed to swell less than those equilibrating at 50°C, although much more creep occurred at 60°C. This could be due to a lesser degree of methanol saturation of nitrogen at 60°C, so that the true activities are slightly lower than stated.

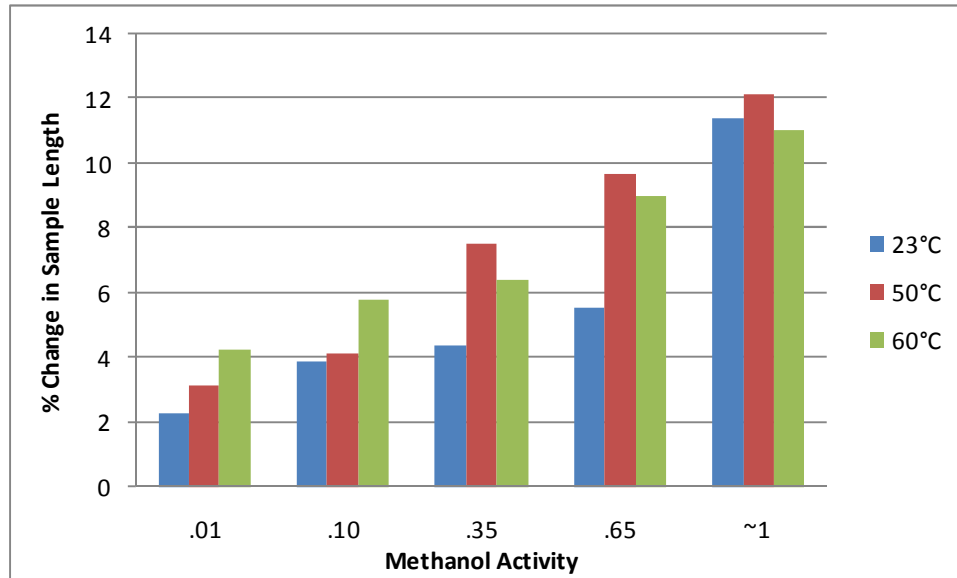


**Figure 4.2 Membrane welling after 12 hours of equilibration in different methanol activities**

Exposing Nafion to methanol vapor results in methanol uptake by the membrane. The increasing swelling strain with methanol activity is due to increased methanol uptake by the polymer. Mass uptake increases the size of the acid clusters as hydrogen bonds are formed between the polar methanol and the hydrophilic sulfonic acid groups. Dimensional swelling is necessary for the Nafion to accommodate the larger solvated acid clusters. Equilibrium mass uptake is a strong function of activity, but only depends weakly on temperature. This was confirmed by the fact that membrane swelling increased consistently with activity, but only a small correlation was seen with temperature.

## **4.3 Nafion® Creep Response in 100% Methanol**

### *4.3.1 Introduction*

Tensile creep was measured at 23, 50 and 60°C for activities 0, 0.01, 0.10, 0.35, 0.65, and ~1. Nitrogen and methanol were supplied through a bubbler at different flow rates to obtain these different activities. Sample width and thickness before creep were 0.25" and 0.01" respectively, and the initial gauge length was 1.00". The applied force for all runs was 1.48 Newtons. The repeatability of the creep apparatus was initially tested by repeating runs. Results were found to be repeatable with an error of around 5%. Additionally, some runs were repeated to confirm specific results.

### *4.3.2 Results*

Results for creep response at room temperature, around 23°C, are given in Figures 4.3a and 4.3b. Creep response increases with activity. The extremes of this result are seen in runs with activity around 0 and 1. Almost no creep occurs for activity ~0, whereas for activity ~1, strain rises above 0.25. Nafion creep can be analyzed in more detail by breaking total creep strain down into its components. Total creep strain, instantaneous elastic creep, delayed elastic creep, and viscous losses were determined for every run. An analysis of creep components at 23 °C is found in Figure 4.3c.

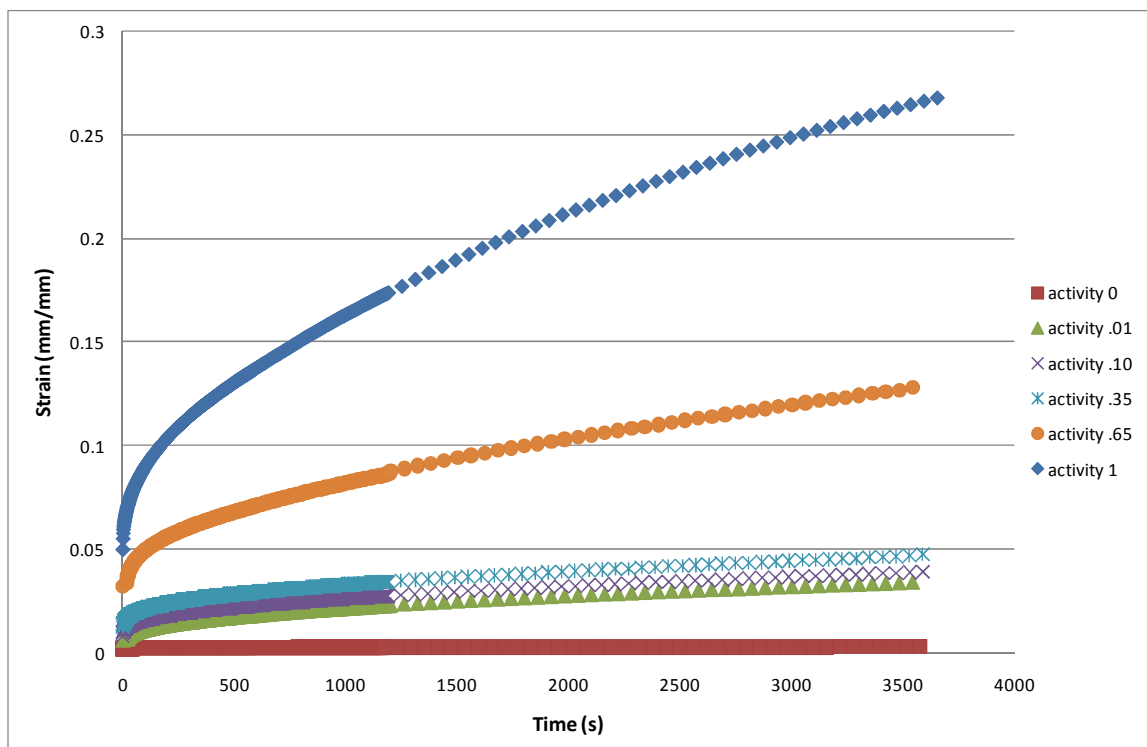


Figure 4.3a Nafion® creep response for different methanol activities at 23°C.

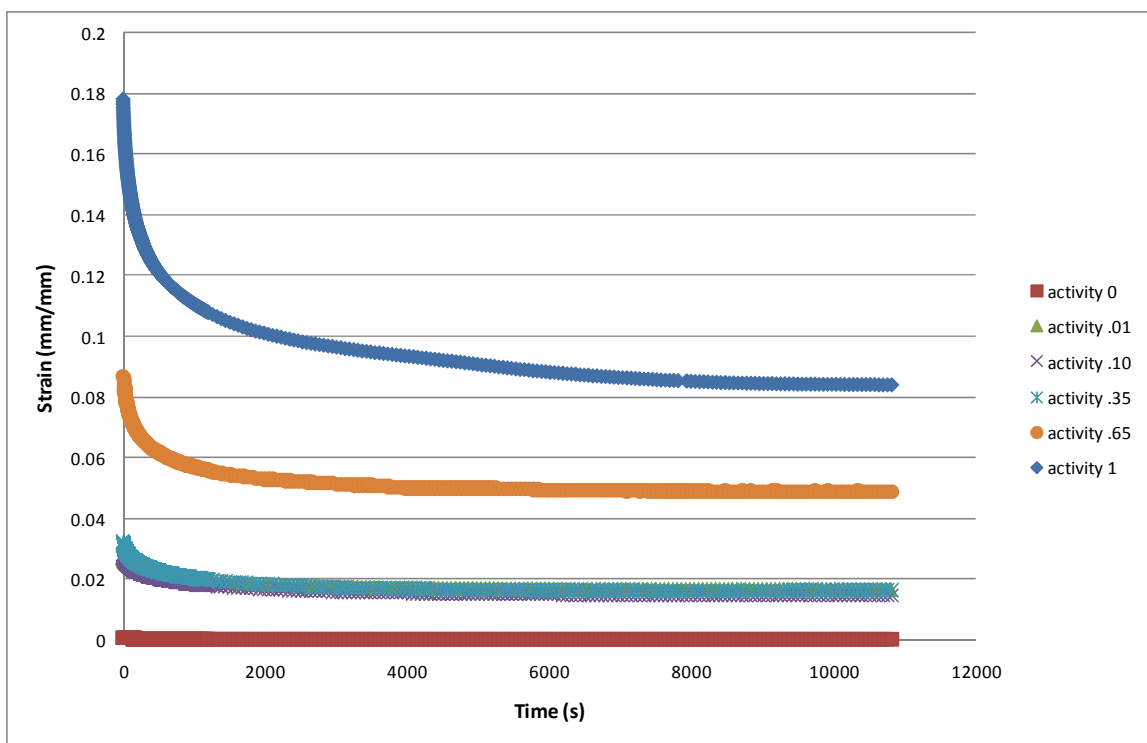
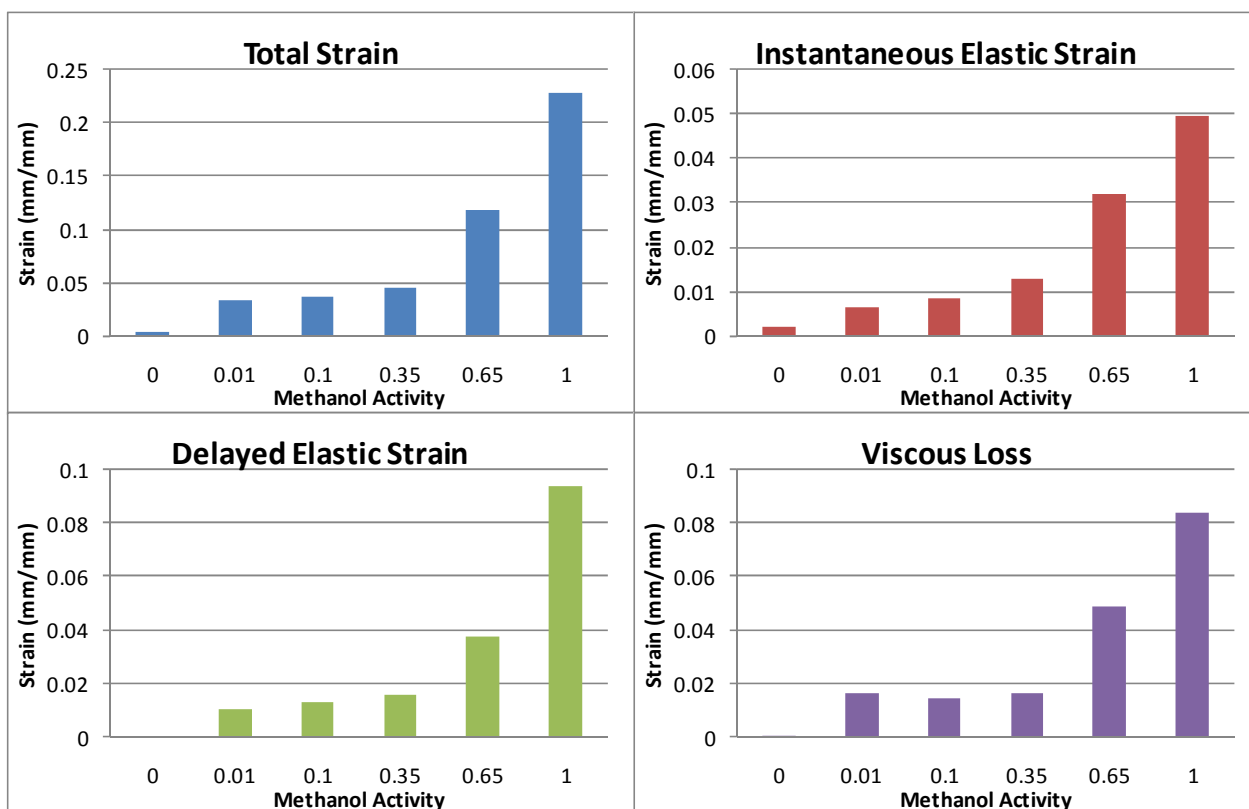


Figure 4.3b Nafion® creep recovery for different methanol activities at 23°C.





**Figure 4.3c** Creep strain and components at 23°C as a function of water activity, associated with runs shown in Figure 4.3a and 4.3b

The experiment was repeated at elevated temperatures of 50°C and 60°C. The boiling point of methanol is 64.7°C, so the experiment cannot be operated too close to this temperature. The results for Nafion® creep and creep recovery at 50°C are given in Figures 4.4a and 4.4b, respectively. Again, the general trend is that creep increases with increased activity. Interestingly, the run for activity 0.10 did not follow this trend at 50 and 60 °C, and showed less creep strain than activity 0.01. At 50 °C, creep strain increased from activity 0 to 0.01, decreased at activity 0.10, and increased again up until activity 1. A similar result was seen at 60°C, except here creep strain for activity 0.10 was even less than that for activity 0. This indicates that there is some type of transition that occurs around activity .10. Results for 60 °C are shown in Figures 4.5a through 4.5c.

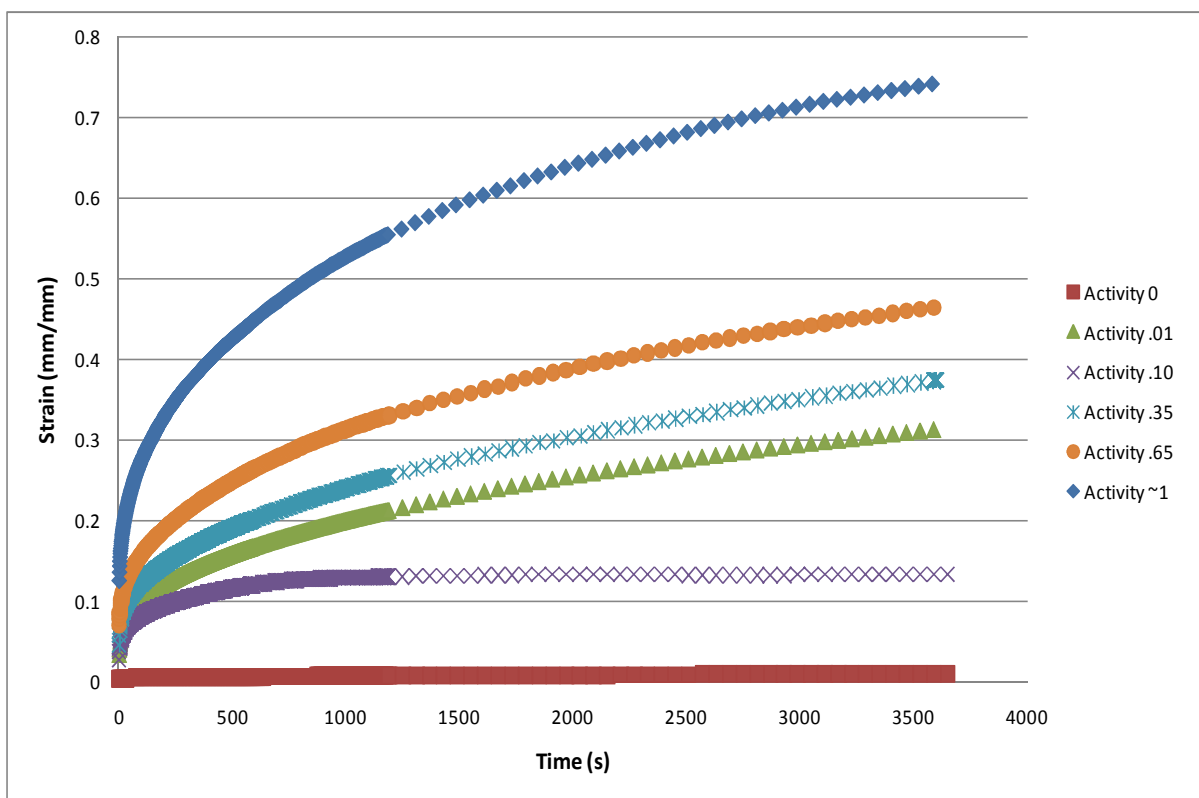


Figure 4.4a Nafion® creep response for different methanol activities at 50 °C

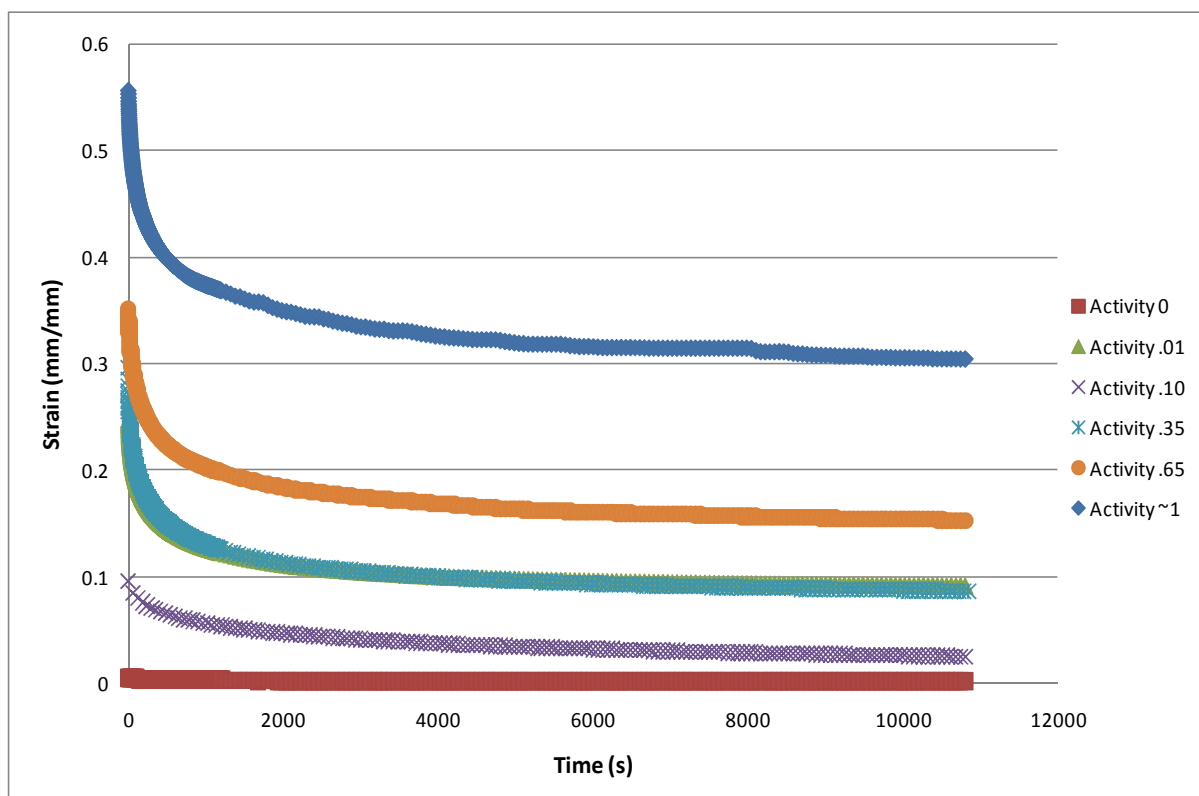


Figure 4.4a Nafion® creep recovery for different methanol activities at 50 °C

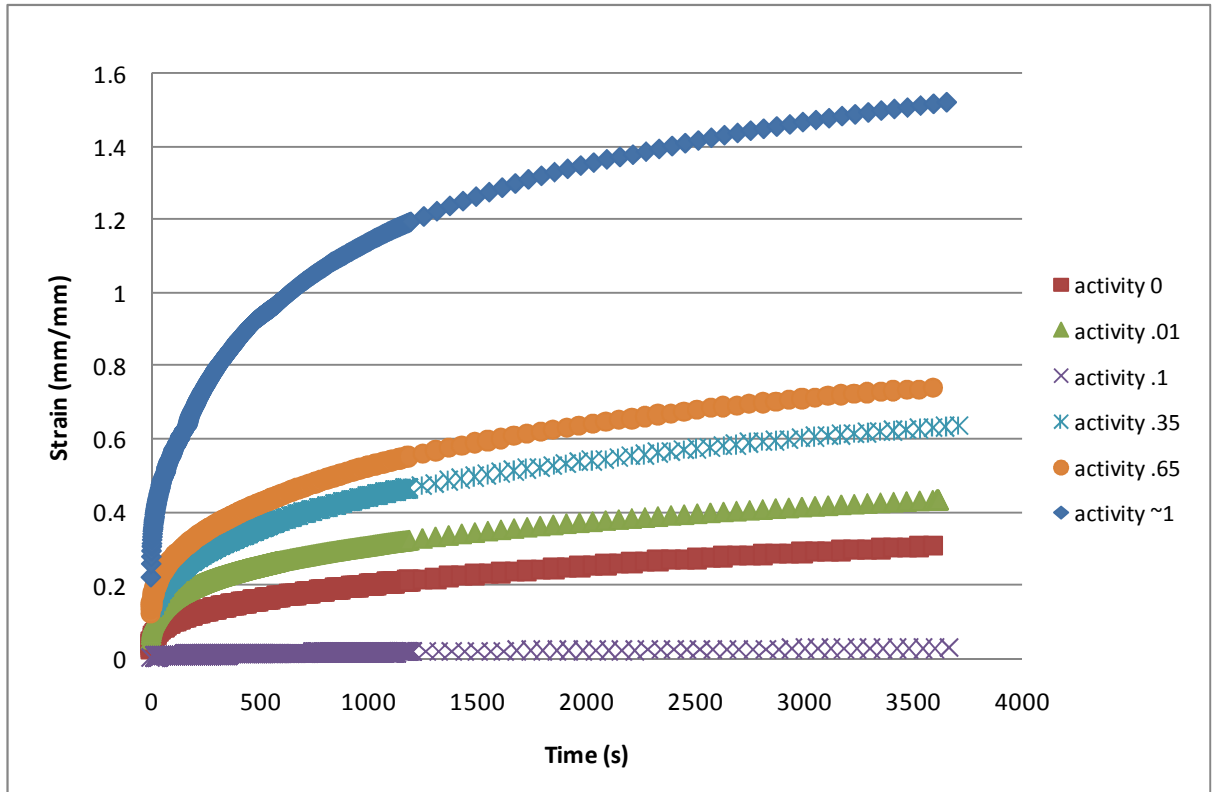


Figure 4.5a Nafion® creep response for different methanol activities at 60 °C

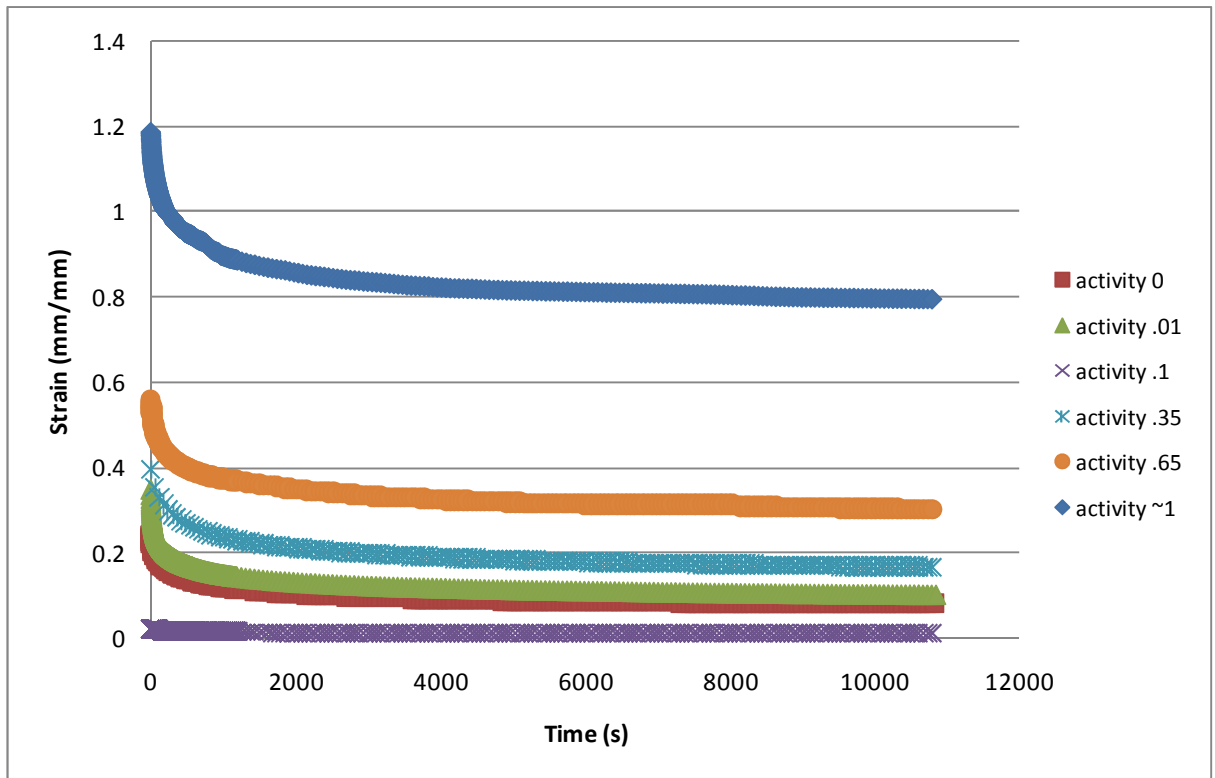


Figure 4.5b Nafion® creep recovery for different methanol activities at 60 °C

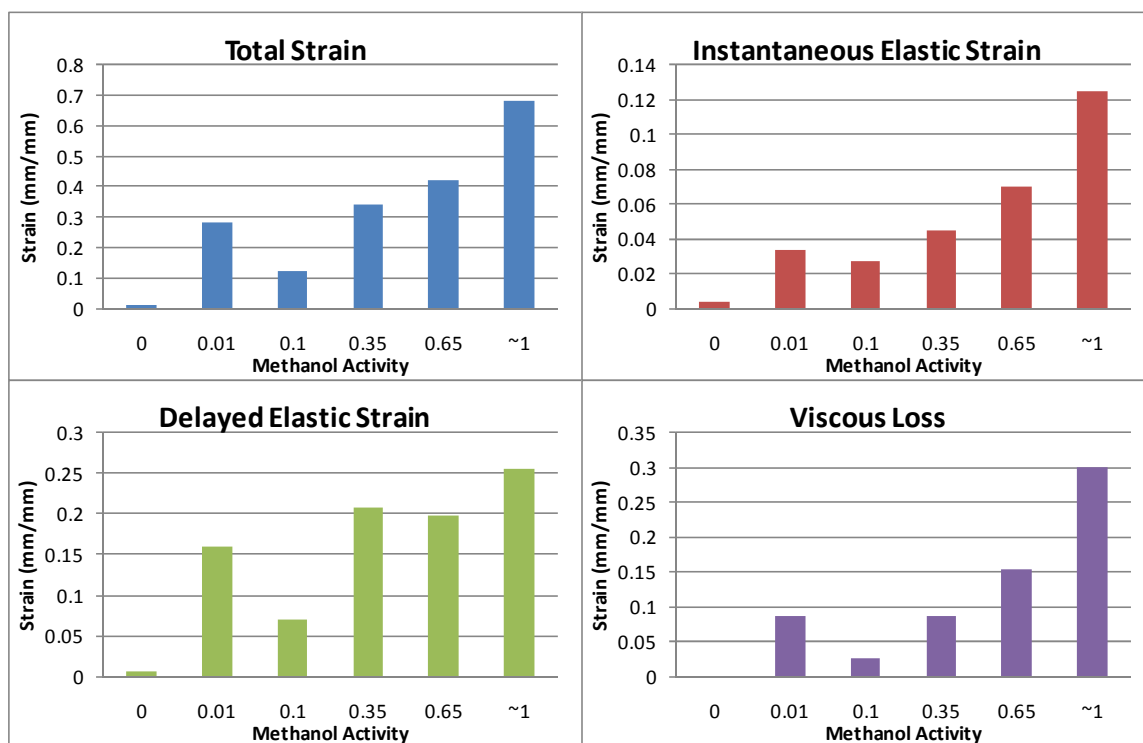


Figure 4.4c Creep strain components at 50°C as a function of water activity, associated with runs shown in Figure 4.4a and 4.4b

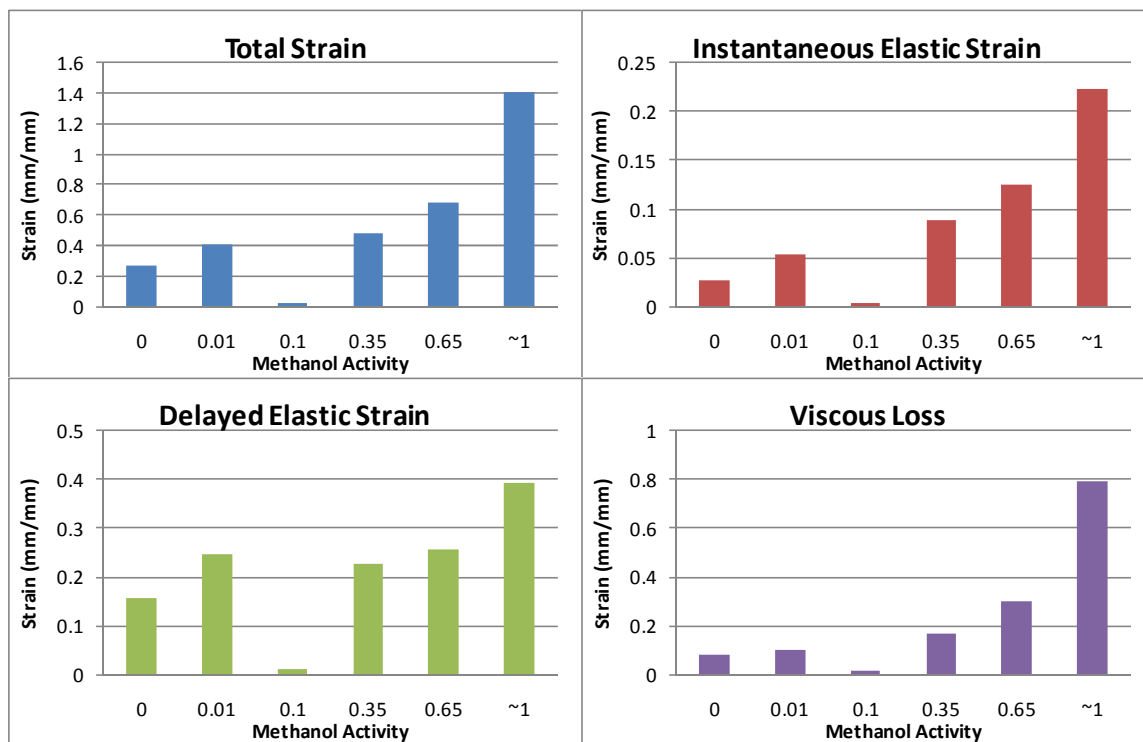
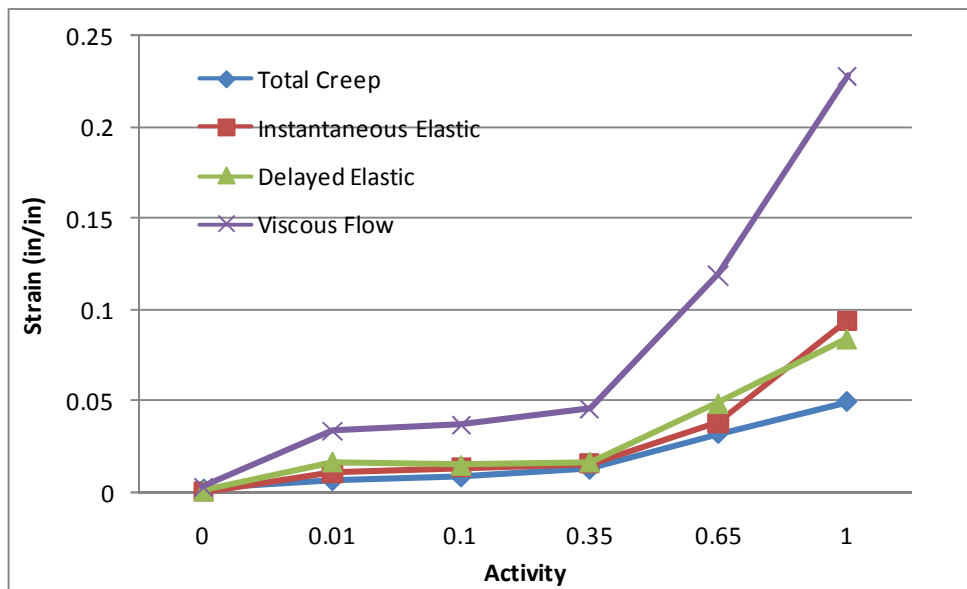
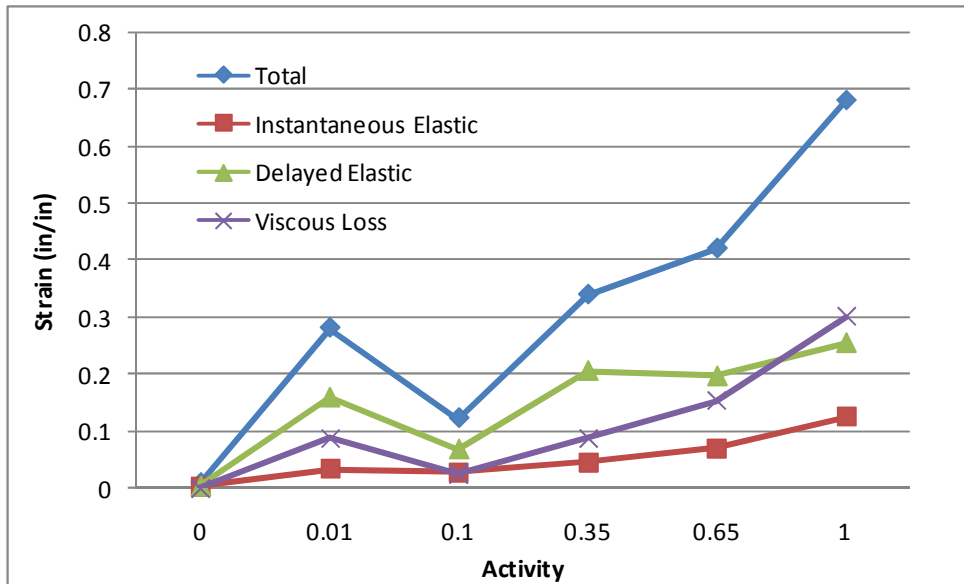


Figure 4.5c Creep strain components at 60°C as a function of water activity, associated with runs shown in Figure 4.5a and 4.5b



**Figure 4.6** Plot of creep strain components at 23°C as a function of methanol activity, associated with runs shown in Figure 4.3



**Figure 4.7** Plot of creep strain components at 50°C as a function of methanol activity, associated with runs shown in Figure 4.4

Additional information can be gained by examining the different creep components separately. Figures 4.6 and 4.7 show a plot of creep strain components at 25°C and 50°C respectively, versus activity. Results for 60°C were very similar to those at 50°C. As expected given the results discussed above, in general all three creep components,  $\epsilon_e$ ,  $\epsilon_d$ , and  $\epsilon_v$ , increase with activity. At higher temperatures, creep components go through a maximum at activity .01, decrease significantly at activity .10, and increases again at higher activities.

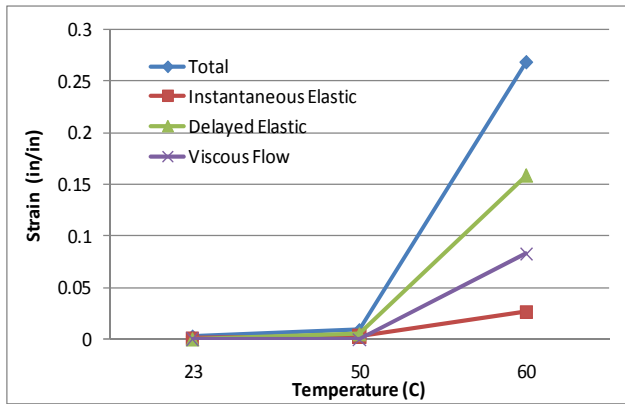


Figure 4.8a Creep strain components vs. temperature at activity 0

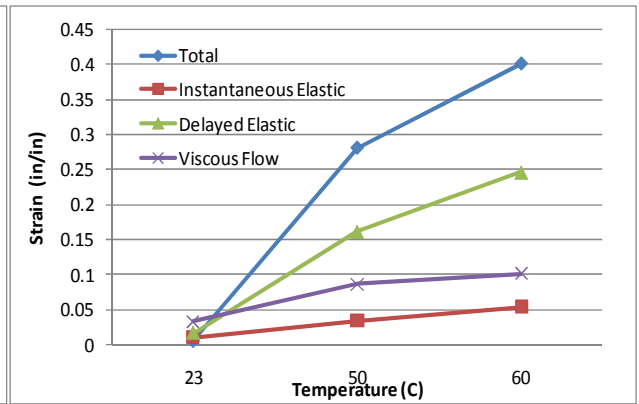


Figure 4.8b Creep strain components vs. temperature at activity 0.01

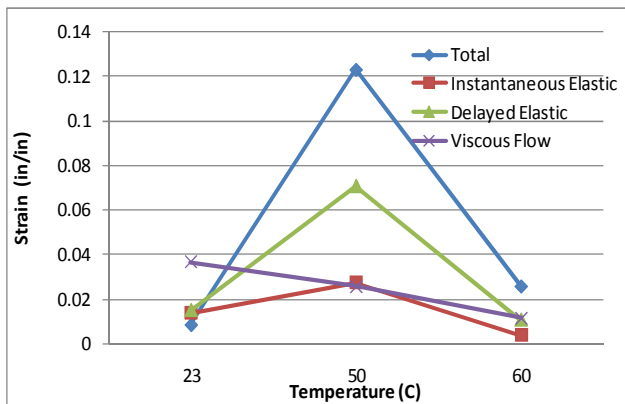


Figure 4.8c Creep strain components vs. temperature at activity 0.10

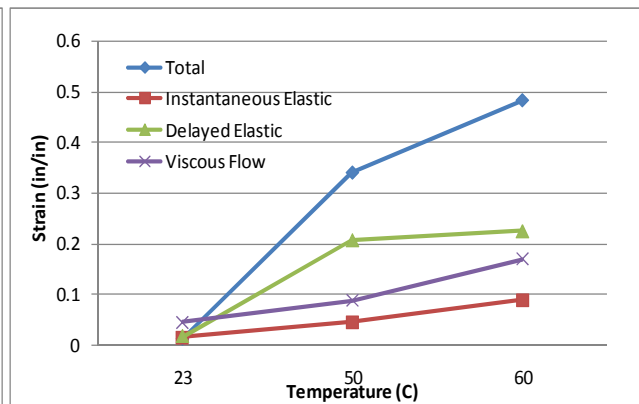


Figure 4.8d Creep strain components vs. temperature at activity 0.35

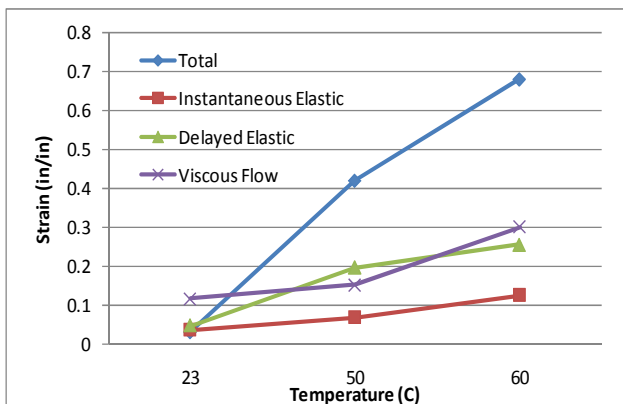


Figure 4.8e Creep strain components vs. temperature at activity 0.65

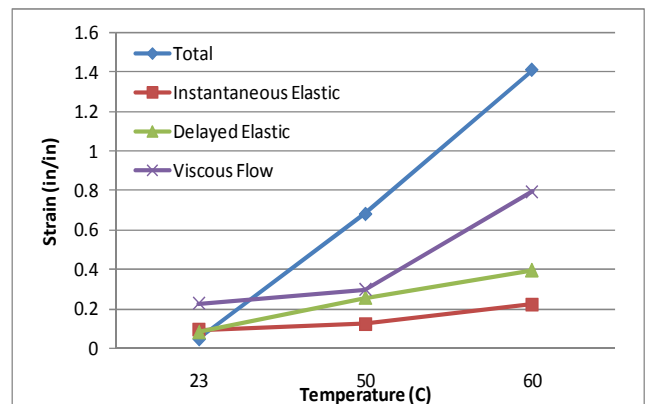


Figure 4.8f Creep strain components vs. temperature at activity ~1

The effect of temperature on creep response can be broken down by looking at the plots of the different creep components against temperature for each different activity. Examining the entire set of plots in Figures 4.8a to 4.8f, it can be seen that in general creep components increase significantly with temperature. The exception to these trends is activity .10, in which creep components exhibit a maximum at 50 °C. There is very little difference in creep components for dry Nafion® between 23 and 50 °C , but a large increase from 50 °C to 60 °C. For all other activities besides 0.10, the different components increased fairly smoothly with temperature. Not including activity 0 and activity .10, as activity increases, the difference in creep components between 23 and 50 °C becomes less significant and the difference between 50 and 60 °C becomes more significant. This can be seen in the plots in the decrease in slope between 23 and 50 °C and the increase in slope between 50 and 60 °C for activities greater than 0.

#### *4.3.3 Discussion*

Both temperature and solvent activity strongly affect the viscoelastic response of Nafion. In general, creep increased significantly with increasing temperature. This is because bonding strength between polymer chains decreases with increasing temperature, and therefore the sample creeps more. However, the combined effects of temperature and solvent activity are complicated, as will be discussed below.

Methanol activity strongly affects the viscoelastic response of Nafion at all temperatures. Explanations will be given for the creep behavior of Nafion based on changes in its microstructure with creep conditions. The introduction of methanol results in changes in the microstructure of Nafion through the acid clusters, teflonic matrix, and bonding between sulfonate groups. Methanol is protic and possesses a hydrophobic tail. The (polar)

protic aspect allows the methanol to undergo hydrogen bonding with sulfonic acid sites, which are also polar. The non-polar hydrophobic tail can sometimes interact with the non-polar teflonic matrix. Methanol also disrupts the bonding between sulfonate groups that are present in dry Nafion due to the formation of stronger hydrogen bonds between methanol molecules and the sulfonate groups.

Generally, tensile creep strain was found to increase with increase in methanol activity for all three temperatures. The exception to this trend was runs for methanol activity 0.10 at elevated temperatures, which showed a very small creep response. This result was found to be repeatable at both 50°C and 60°C. As temperature increases, creep at activity .10 seems to decrease relative to the other activities at that temperature.

Dry Nafion at 23 °C, exhibited an almost negligible amount of creep. The high stiffness and resistance to creep of dry Nafion at room temperature is attributed mostly to cross-linking between the sulfonic acid groups (Majsztrik, 2007). The reason dry Nafion begins to creep more at 50 and 60 °C is that at higher temperatures these cross-links are overcome by thermal kinetic energy. The fact that viscous loss and delayed elastic strain increase significantly at 60 °C provides further evidence to support this. As the dry Nafion is exposed to methanol, the polymer is plasticized, and creep increases with activity.

The general increase in creep strain with methanol activity may be explained in terms of changes in free volume. Free volume is associated with the space between molecules in a material. Exposing Nafion to methanol *increases* free volume due to methanol's interaction with both the sulfonic acid clusters and the teflonic matrix. This can be seen as having the opposite effect of elevated drying temperature, which decreases free volume. As will be discussed in Section 4.3, elevated drying temperature has an “annealing”



effect, which results in decreased free volume because of denser packing of Nafion's® side and main chains (Mauritz, 2004). The addition of methanol has the opposite effect, to increase free volume and thus increase the mobility of side chains. If side chains are more mobile, the sample will creep more. This explains the general increase in creep strain in Nafion with activity. This hypothesis for Nafion creep in the presence of methanol is similar to that of Majsztrik for creep in water at room temperature (Majsztrik, 2007).

Creep increased significantly at activities 0.65 and ~1. This is may be due to interactions between methanol and the hydrophobic backbone of Nafion. Like water, methanol will interact mostly with the ionic acid clusters due to its polar –OH group. But unlike water, under a highly swollen state methanol is also capable of interacting with the hydrophobic matrix due to its hydrophobic –CH<sub>3</sub> group. This was shown in an IR spectroscopy study of Nafion which found hydrogen bonding interactions between methanol and –CF<sub>2</sub>, part of the hydrophobic backbone (Tsai and Hwang, 2007). The study specified that this interaction occurs only under a highly swollen state, and thus at high methanol activities (Tsai and Hwang, 2007). At higher activities such as 0.65 and ~1, the interactions between Nafion and methanol increase free volume through both the acid clusters and the teflonic backbone. This results in a larger increase in creep strain at these high activities.

Perhaps the most interesting result found was the unusually small creep that occurred around activity .10 at 50 and 60°C, indicating that there may be some structural changes occurring in Nafion® around these conditions. Before we discuss the explanation behind the results found, it is helpful to consider a similar study conducted on tensile creep of Nafion in the presence of water, given in Figure 4.9 (Majsztzik, 2007). As with methanol, at 23°C, it was found that water plasticizes Nafion and creep increases with water activity.

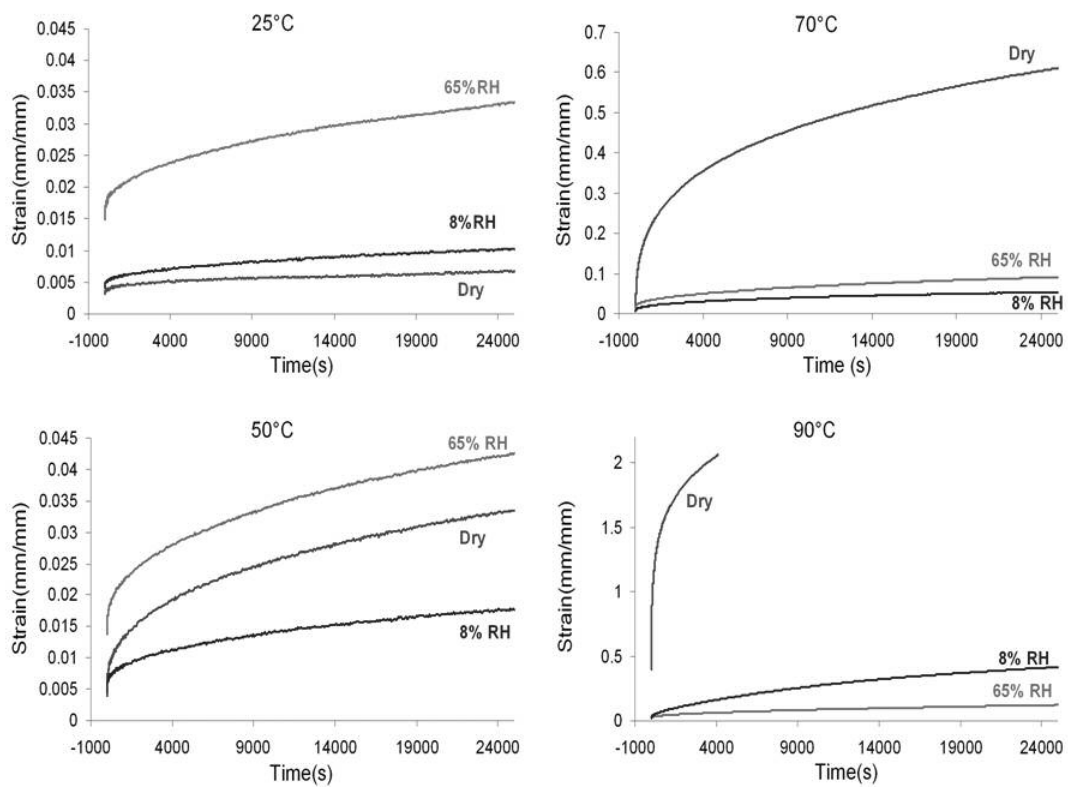


**Figure 4.9 Nafion creep response for different water activities and temperatures (Majsztzik, 2007)**

Interestingly, creep at 90°C shows the opposite trend: creep *decreases* with hydration at 90°C. At the intermediate temperatures 50 and 70°C, creep strain exhibits a local maximum at intermediate water activities.

A similar result is seen with methanol at intermediate temperature; the position of the local maximum with solvent activity has simply shifted. At 50 and 60 °C, a very pronounced local maximum in creep strain occurs at methanol activity .01. Thus, the maximum occurs at a much lower activity than that for water. This shift is due to the fact that for any given activity, methanol has a greater effect on the morphology of the membrane because more methanol enters the membrane than water. This is supported by the fact that methanol produces more swelling in Nafion than water (Benziger, 2008).

The results in both methanol and water can be explained by solute induced changes of the microphase separation in Nafion. As temperature and solute activity change, the hydrophilic microphase restructures itself, as discussed in Section 2.2. The possible equilibrium phases for Nafion are a disordered phase, a BCC cluster phase, a hexagonal cylindrical phase, and possibly a lamellar phase. These phases can be seen in Figure 4.10, a phase diagram developed by Matsen and Bates (2004), and adapted by Benziger et. al (2008). Transitions corresponding to temperature are vertical lines, while transitions corresponding to changes in water activity at constant temperature are lines that move up and to the right. It is suspected that changes in methanol activity correspond to lines that move slightly down and to the right, as indicated by the red line Figure 4.10.

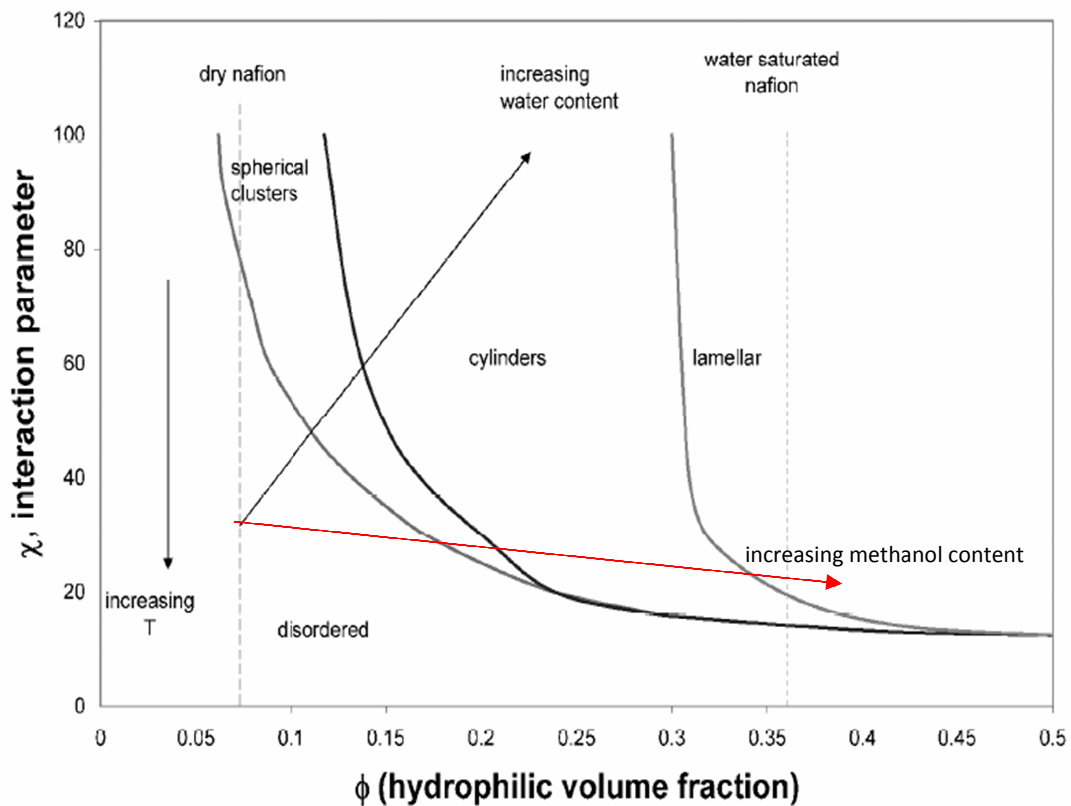


Figure 4.10 Phase diagram for microphase separation in block copolymers (Benziger, 2008)

Absorption of a solute such as water or methanol will alter the volume fractions of the two phases and the interaction parameter between them. Water makes the phases separate more, while methanol increases the strength of the interaction between the two phases, or at least moderates the interaction between the two phases. This is due to the fact that methanol possesses both a hydrophilic  $\text{-OH}$  group and a hydrophobic  $\text{-CH}_3$  group, so that it can interact with both phases. This is why the lines corresponding to increasing methanol and increasing water activity move in different directions.

For dry Nafion or at very low methanol activity (such as .01), we start in the cluster phase, and as temperature increases, we follow a vertical line downwards. As temperature increases, the sulfonic acid groups will break up and randomly distribute themselves in the

continuous TFE phase (Benziger, 2008). This state is referred to as the disordered phase. The sulfonic acid groups disrupts the crystalline structure which causes an increase in creep rate, since creep is dominated by the TFE phase. This is the reason that creep for dry Nafion or very low methanol activities increases with temperature.

Around methanol activity .10, microstructure is probably in the spherical clusters region. This system remains phase separated. Since the sulfonic acid groups are phase separated from the TFE in this phase, the TFE's crystalline structure is preserved, and the sample actually creeps less than dry Nafion® at the same temperature. As activity is increased further, the microphase evolves into the cylindrical phase, and at very high activities into the lamellar phase. In these regions, phase separation is no longer so distinct, especially in the lamellar phase, causing creep to increase again. Thus, creep continues to increase with activity up to an activity of around one.

## 4.5 Thermal History Effects

### 4.5.1 Results

Tensile creep runs were carried out to determine the effects of Nafion's® thermal history on its mechanical properties. This was done by varying the time and the temperature of the drying step. The standard drying procedure for the creep runs in this thesis was to dry for 3 hours at 50 °C . For comparison, Nafion® was also dried at 50 °C for 12 hours, and at 100 °C for both 3 and 12 hours. Following drying, the samples were cooled to the test temperature of 23 °C and underwent the standard creep testing for activities 0, 0.10, and 0.65. Results for creep and creep recovery are shown in Figures 4.11 through 4.13.

For the dry runs, drying at 100 °C resulted in significantly higher creep strain than drying at 50 °C. It may be difficult to see in the figures because of the low creep strains involved, but total creep for dry Nafion after drying for 3 hours at 100 °C was a factor of five times larger than that for drying at 50 °C. This factor was even higher for drying for 12 hours. For the runs at methanol activity 0.10 and 0.65, the opposite result was seen. Drying at the higher temperature resulted in a lower creep strain than in samples dried at the lower temperature. At methanol activity 0.65 , total creep strain for the sample dried at 50 °C was 4 times greater than that for the sample dried at 100 °C. Results can also be seen in Figure 4.11, which presents an analysis of the differences in creep components for all drying conditions. These results are consistent with the 2007 findings of Majsztrik for Nafion® creep in the presence of water.

It was found that drying for longer periods (12 hours versus 3 hours) caused creep to increase. The largest effect was for activity 0.65, where total creep increased about threefold when dried for 12 hours for drying at both 50 and 100 °C. This can be seen in the

creep component analysis for all the different drying conditions found in Figure 4.11. Drying for 12 hours (blue and red bars) consistently produced more creep for all components than drying for 3 hours (purple and green bars). For the 12 hours runs, it appears that the larger total strain after drying at 50°C is mostly due to an increase in delayed elastic strain and viscous loss.

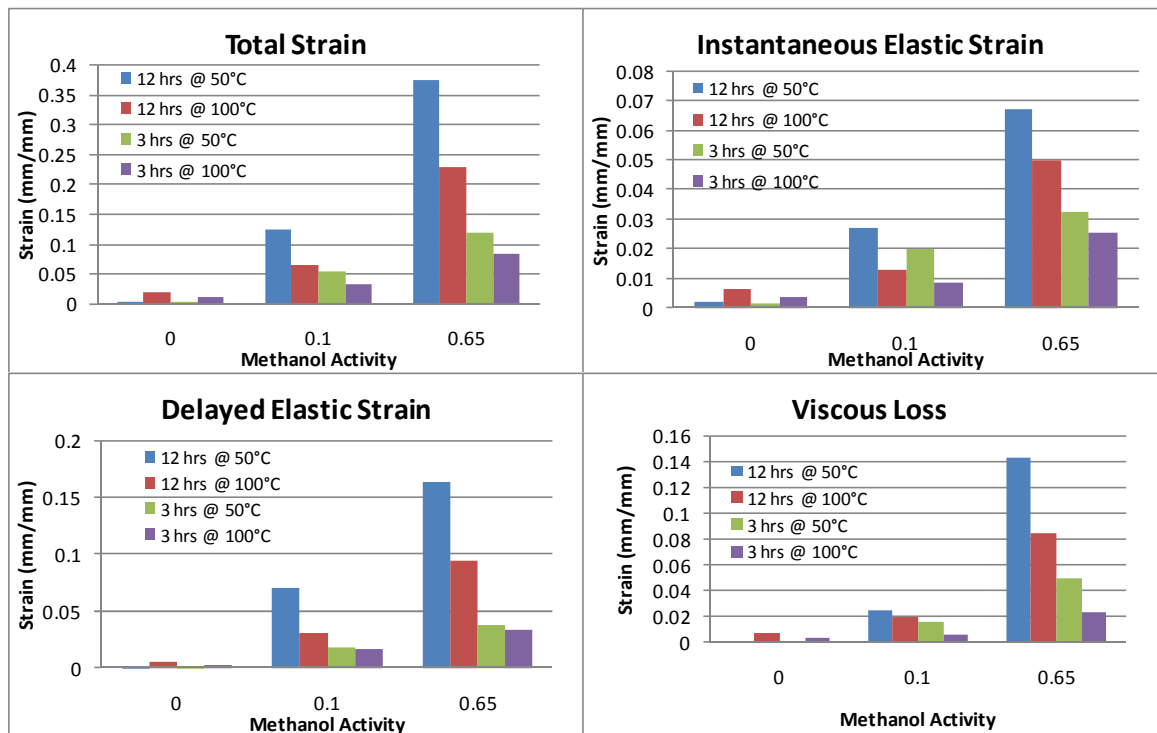


**Figure 4.11** Creep strain components at 23°C as a function of methanol activity for different drying conditions, associated with runs shown in Figures 4.12 and 4.13

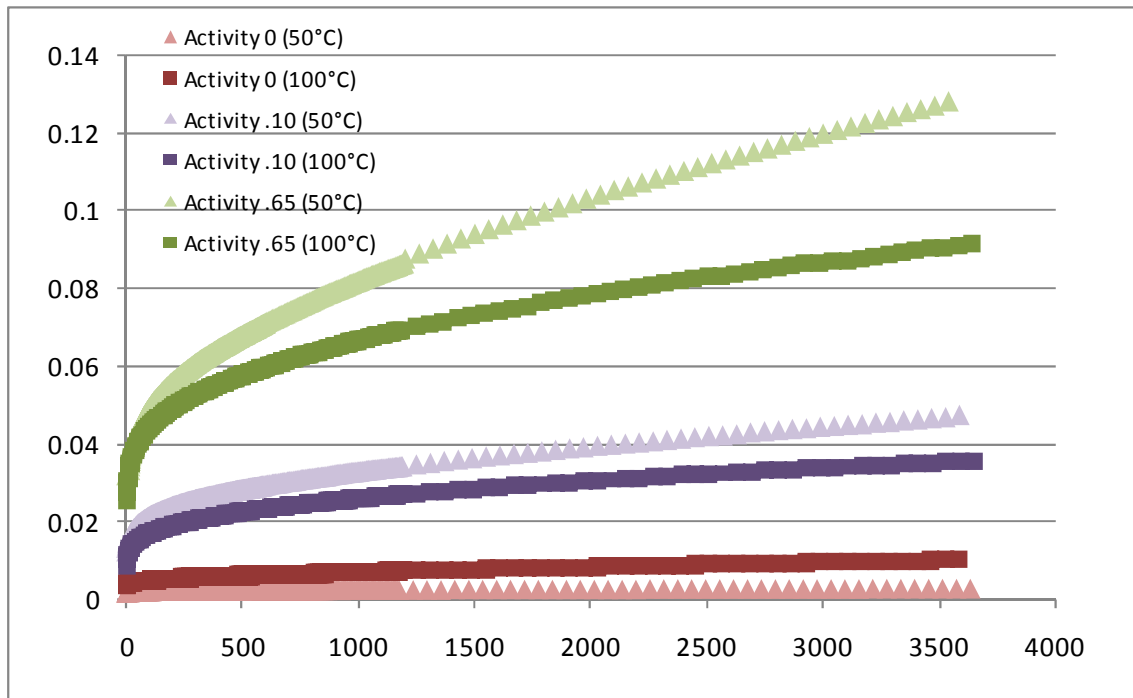


**Figure 4.12a Nafion creep response at 23 °C for different activities and drying temperatures (dried for 3 hours)**

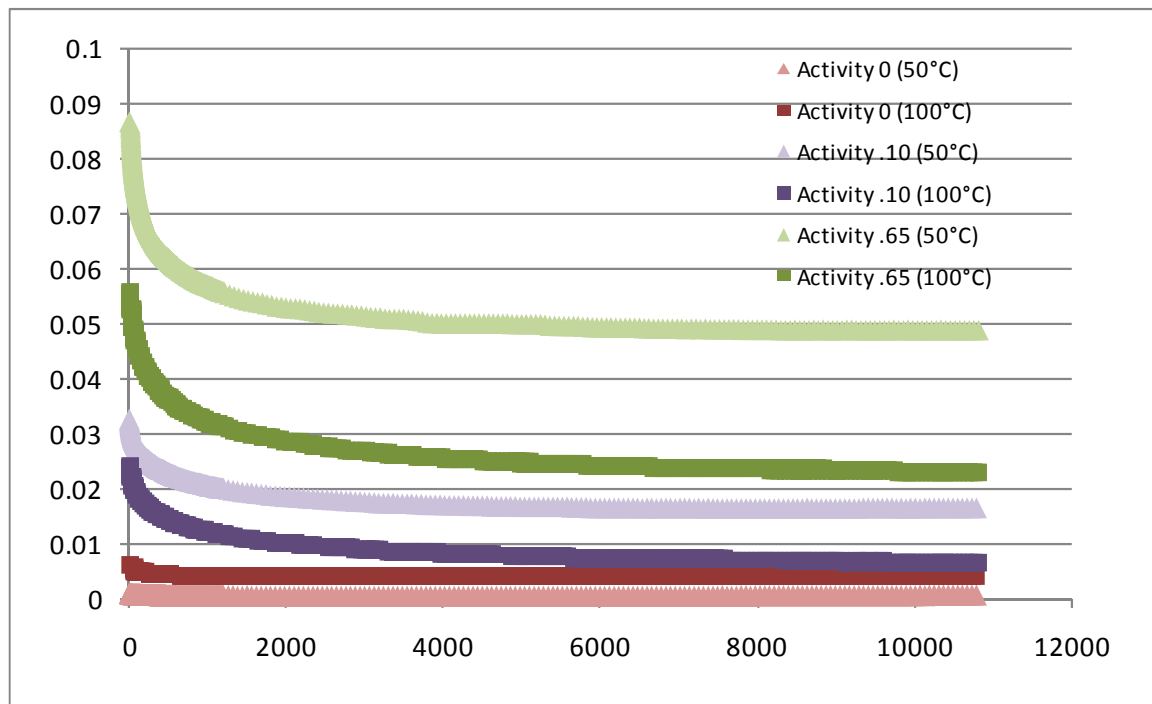


**Figure 4.12b Nafion creep recovery at 23 °C for different activities and drying temperatures (dried for 3 hours)**



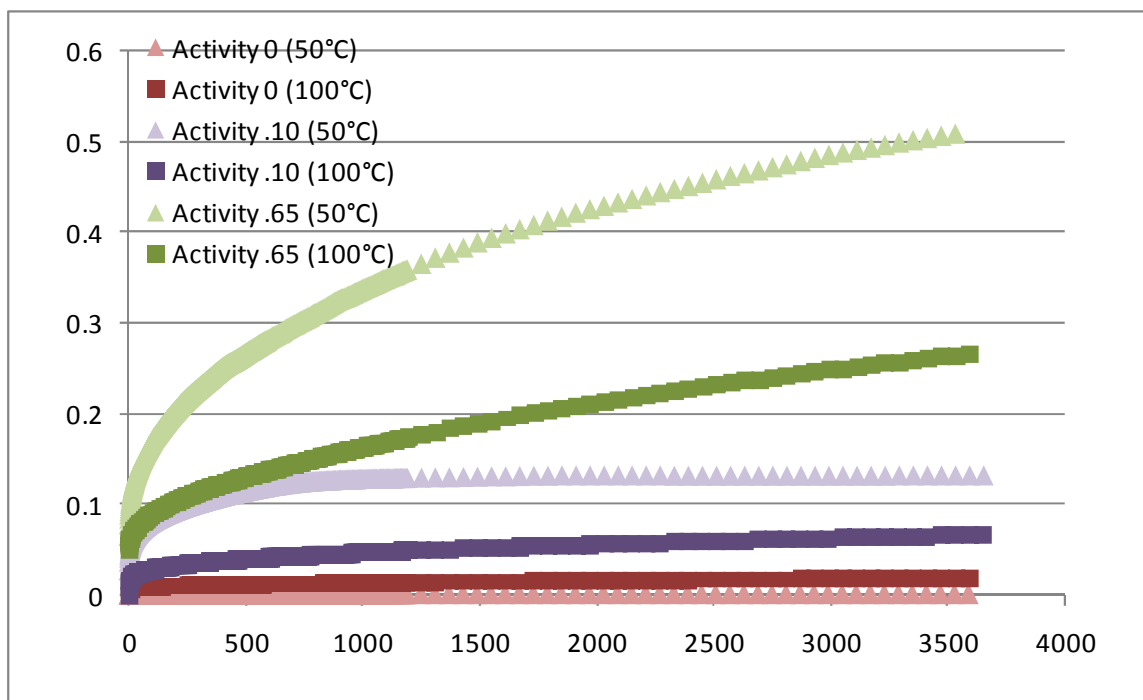


Figure 4.13a Nafion creep response at 23 °C for different activities and drying temperatures (dried for 12 hours)

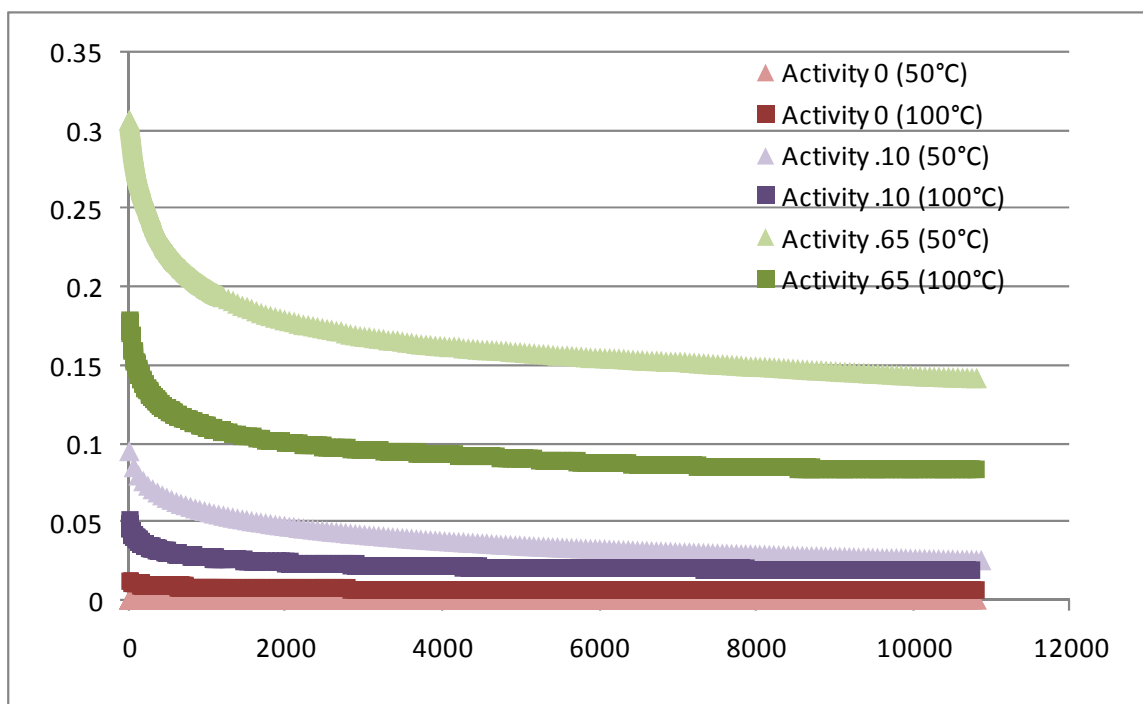


Figure 4.13b Nafion creep recovery at 23 °C for different activities and drying temperatures (dried for 12 hours)

#### 4.5.2 Discussion

The results at activity 0 can be explained in terms of bonding within Nafion. In dry Nafion, ionic groups interact through the electrostatic attraction of S-O-H-O-S groups, resulting in polymer cross-linking. It is suspected that cross-links between side chains give dry Nafion® its high resistance to creep at 23 °C (Majsztrik, 2007). Majsztrik suggests that between 50 and 80 °C the strength of this bond is thermally deactivated. Therefore drying at 100 °C will increase creep at 0 methanol activity because it significantly weakens the cross-links which normally give dry Nafion® its resistance to creep strain

For activities 0.10 and 0.65, a different effect is seen, due to the introduction of methanol. The results can be explained in terms of cluster sizes in Nafion®, where the term cluster is used to describe the hydrophilic domains within the phase-separated polymer. It has been proposed that high temperature drying results in smaller clusters (Hinatsu, 1994). Further explanation is offered by Mauritz and Moore: that the decreased volume of clusters is due to denser packing of side and main chains and microstructure (Mauritz, 2004). In their 2007 study on the effects of thermal annealing on Nafion®, Hensley et. al. found that larger clusters will result in higher equilibrium water uptake in a Nafion® film (Hensley, 2007). It is reasonable to infer that larger clusters will result in larger methanol uptake as well. This thesis has shown that at 23 °C, creep strain increases with methanol activity, and thus with methanol uptake. As discussed above, elevated drying temperature results in smaller acid clusters, and therefore smaller methanol uptake. If methanol uptake is decreased, as in those samples dried at 100 °C, it is reasonable to assume that creep strain will be decreased as well.

The results for drying time may be explained by microphase restructuring in Nafion. This process is a mixture of both thermodynamics and kinetics, thus, it is a time dependent process. If the membrane is dried for a longer period of time, it becomes more disordered. As the membrane is cooled back down, it begins to revert back towards its original state, however, since the membrane was dried for such a long period of time, it also takes a long time to revert back. Therefore the sample is not as stiff, and more creep occurs. This effect is greater for higher temperatures.

#### **4.5 Solvent Effects**

The tensile creep response of Nafion<sup>®</sup> was investigated using a 50/50 mixture of methanol and water by mol fraction. This was done mostly to examine the synergistic effects of methanol and water on creep response. However, it also provides a method to probe deeper into the interactions occurring in Nafion<sup>®</sup> which give it its unique mechanical properties. Results for the methanol-water mixture are also compared to results with pure methanol, as well as those with pure water, courtesy of Majsztrik (2007). Volumes were calculated to achieve the desired activity based on the assumption of Raoult's Law in vapor-liquid equilibrium.

Creep strain curves for the methanol/water mixture at 23 and 60 °C are given in Figure 4.15 and 4.16, respectively. For comparison, results from Majsztrik's 2007 study of Nafion<sup>®</sup> creep at 23°C and 50°C when exposed to water vapor are presented in Figures 4.17-4.18. Unfortunately, there are no results for water at 60°C, although general comparisons can be made at these intermediate temperatures. The creep behavior for methanol seen at 23 °C is as expected, creep increases with increasing activity. Comparing creep at room temperature for pure methanol, the 50/50 mixture, and pure water, we see that creep is

very similar for pure methanol and for the methanol/water mixture (See Figure 4.14). We notice that a very similar amount of creep occurred at lower activities for pure methanol and pure water. However at activities .65 and ~1, more creep occurred for methanol than water.

Interestingly, at 60°C, creep was highest for dry Nafion and lower when methanol was introduced. However, creep still increased with increasing methanol activity, although the curves were very close. This inversion is similar to the results seen for pure water at 50 and 70°C by Majsztrik. Total strain for 100% methanol, 50% methanol/50% water, and 100% water at 23°C is reported in Figure 4.14. Results at 60°C for methanol will not be directly compared to those for water, as we only have results for water at 50 and 70°C.

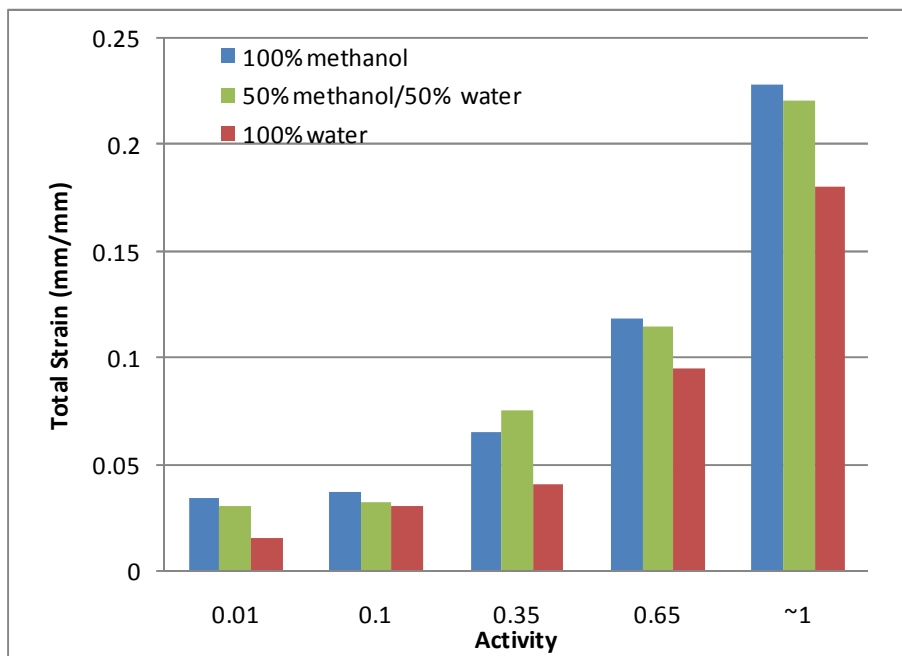


Figure 4.14 Comparison of total creep strain at 23°C for the three solvent types

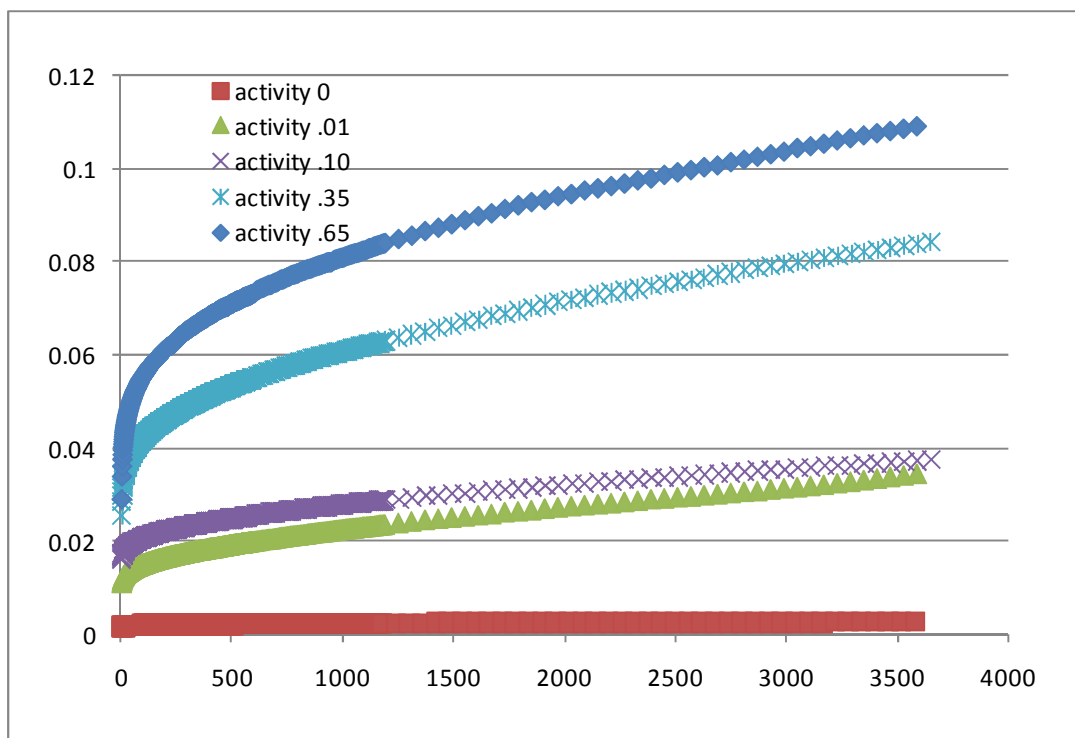


Figure 4.15a Nafion creep response at 23 °C for 50/50 methanol/water mixtures (by mol fraction)

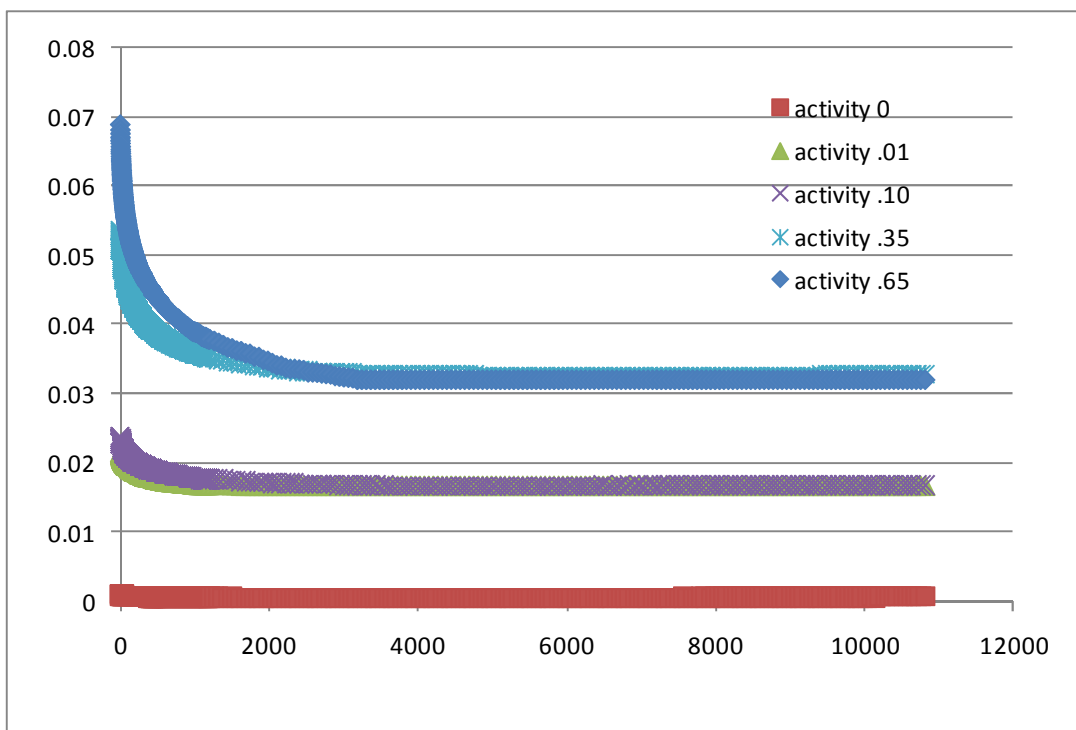


Figure 4.15b Nafion creep recovery at 23 °C for 50/50 methanol/water mixtures (by mol fraction)

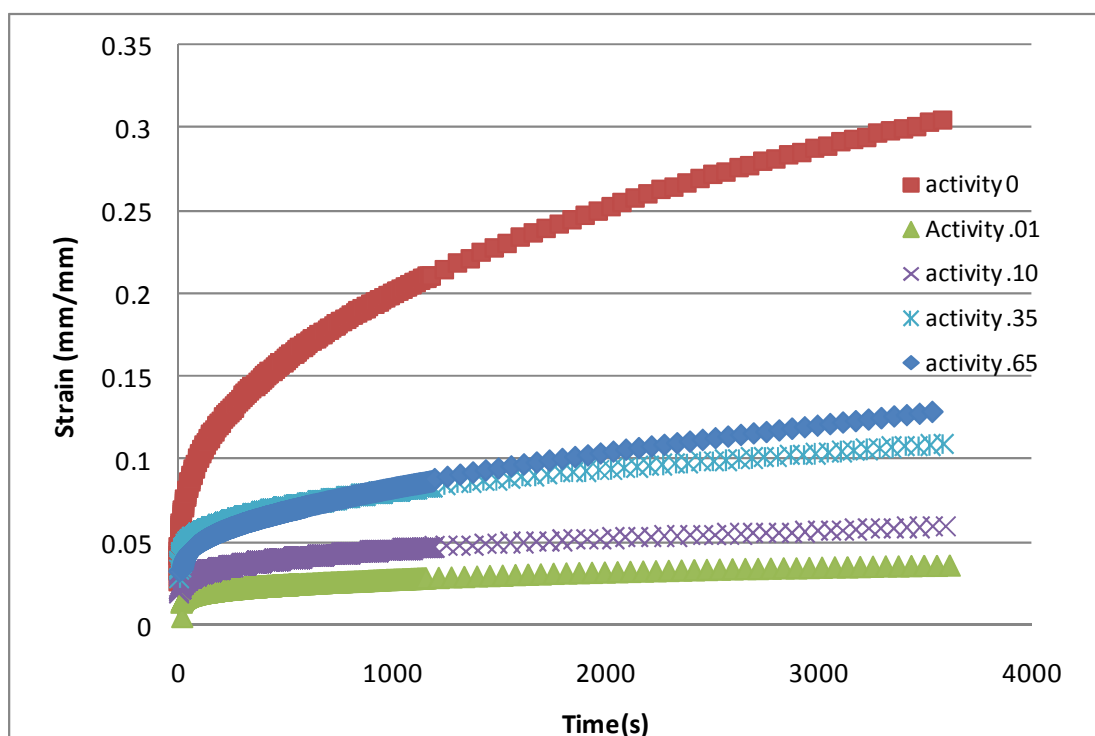


Figure 4.16a Nafion creep response at 60°C for 50/50 methanol/water mixtures (by mol fraction)

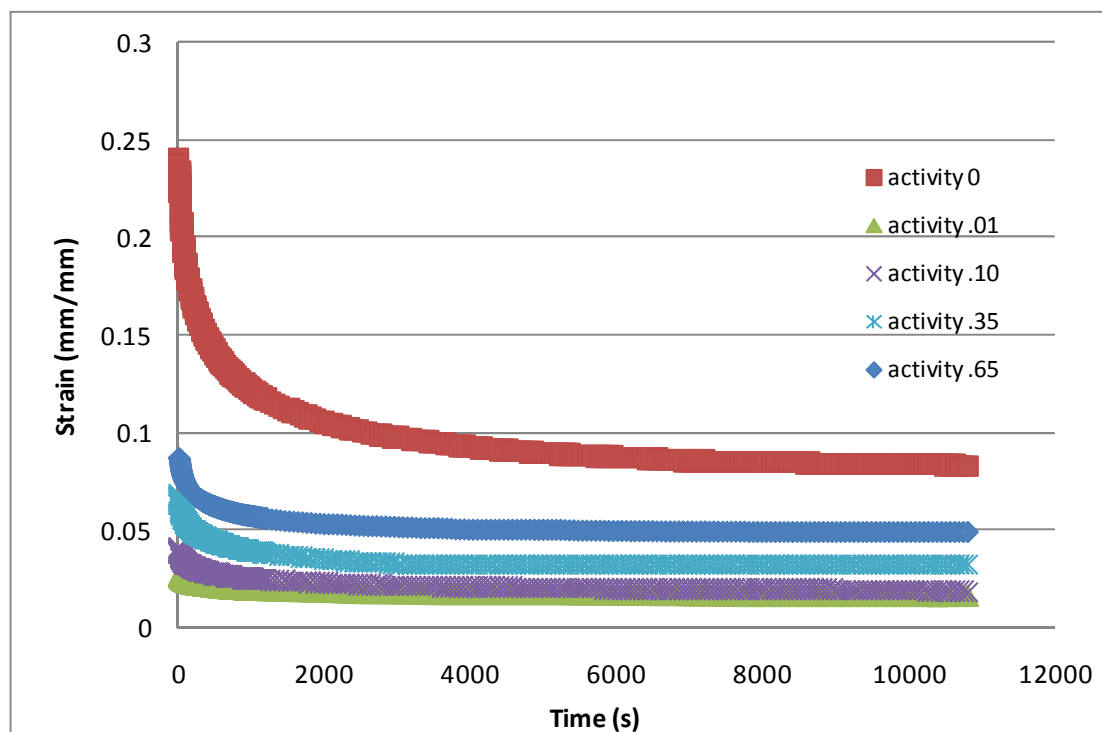


Figure 4.16b Nafion creep recovery at 60°C for 50/50 methanol/water mixtures (by mol fraction)

Creep strain at room temperature is higher for pure methanol and methanol/water mixtures, and lower for pure water. These results can be explained by the differences in interactions between Nafion<sup>®</sup> and the different solvents. Interaction between water and Nafion<sup>®</sup> is restricted entirely to the polar acid clusters as opposed to the non-polar matrix, because water is highly polar. When methanol enters the Nafion<sup>®</sup>, it will also preferentially interact with the hydrophilic acid domains because of its polar -OH group. However, unlike water, under a highly swollen state methanol is also capable of interacting with the hydrophobic matrix due to its hydrophobic -CH<sub>3</sub> group. An IR spectroscopy study of Nafion found hydrogen bonding interactions between methanol the deprotonated sulphonic group in the hydrophilic domains at low methanol activities and with -CF<sub>2</sub>, part of the hydrophobic backbone, at higher activities. (Tsai, 2007). These results are also supported by the fact that methanol produces more swelling than water (Majsztrik, 2007).

The fact that methanol/water mixtures behaved very similarly to pure methanol, especially at higher activities, could be due to the preferential uptake of methanol. Studies found that at low methanol concentrations the uptake of methanol is little affected by the uptake of water, but at higher methanol concentrations the water starts to become excluded (Skou, 1997). At these higher activities, the membrane is becoming mostly saturated with methanol, and therefore behaves as it would if it were exposed to pure methanol.

The results at 60 °C provide further support the theory of microphase separation in Nafion. The result seen here is very similar to that seen for water at 50 and 70 °C. Unfortunately, there are no results for Nafion creep in water at 60 °C for an exact comparison. However, the inversion at intermediate temperatures for dry Nafion and the

local maximum with solute activity is seen. This may be seen as a shift in the temperature of the local maximum seen with solute activity, or a shift in the activity of the local maximum itself.

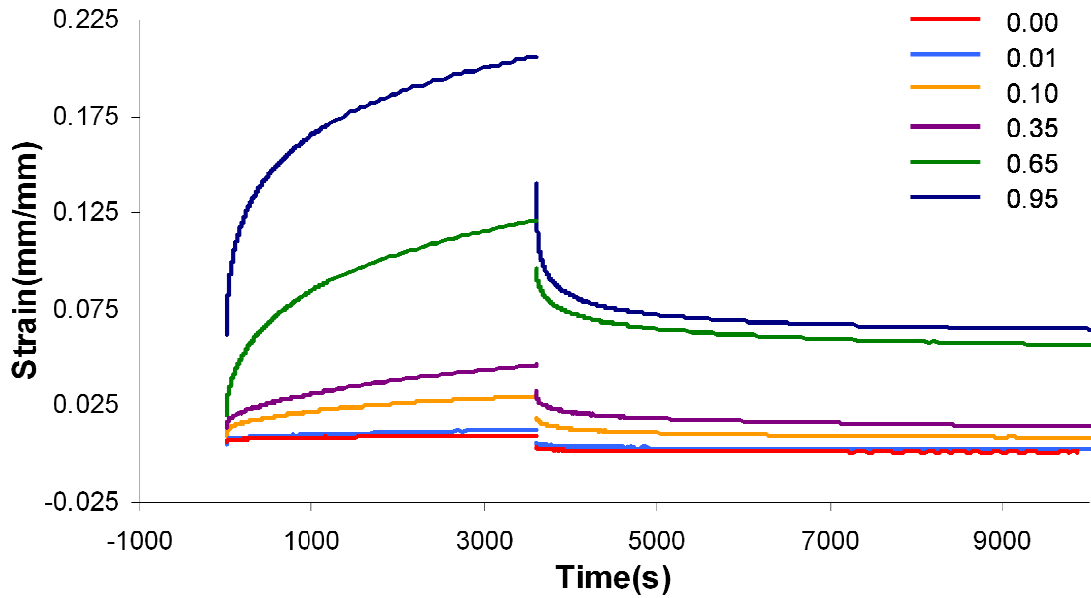


Figure 4.17. Nafion® creep response at 23°C for various water activities. (Courtesy of Majsztrik)

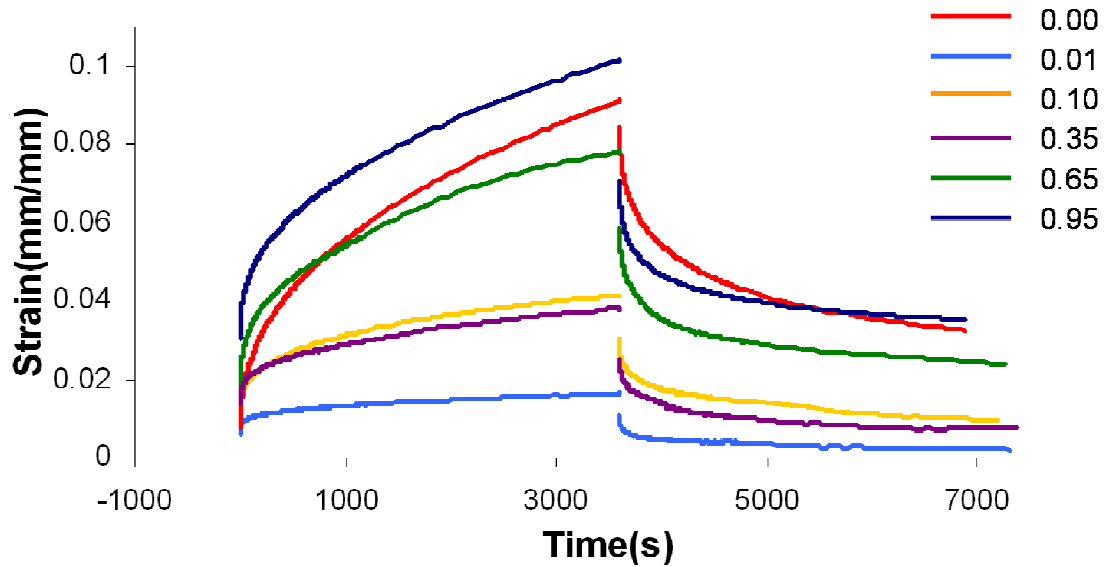


Figure 4.18. Nafion® creep response at 50°C for various water activities. (Courtesy of Majsztrik)



## 5. Conclusion

An understanding of a fuel cell membrane's mechanical properties is essential for improved performance and longevity of a PEM fuel cell. Nafion's® mechanical properties depend strongly on temperature and solvent activity, and thus, the viscoelastic response of Nafion® was investigated at controlled temperature and solvent activity. Tensile creep and membrane swelling were measured using a unique apparatus constructed by Paul Majsztrik which allows creep measurements to be taken at precisely controlled temperatures and solvent activities. The effects of thermal history and different solvents on creep were also investigated.

In general, increased temperature increases creep by decreasing the bonding strength between polymer strains. However, the combined effects of temperature and solvent activity are more complicated. It was shown that at room temperature, increased methanol activity increases creep. Methanol interacts with both sulfonic acid sites and the teflonic backbone of Nafion, which affects the polymers microstructure and bonding interactions. The increase in creep with activity is due to the increased free volume which occurs with the addition of methanol, and thus increased mobility of side chains, which causes more creep to occur. The significantly higher creep strain that occurred at high methanol activities is suspected to be due to the interaction between methanol's non-polar  $-\text{CH}_3$  group and the hydrophobic teflonic backbone of Nafion.

At intermediate temperatures 50 and 60 °C, a local maximum in creep was seen at methanol activity .01. Creep then decreased significantly at activity .10 and increased thereafter. These results are actually similar to those found by Majsztrik for Nafion creep in water, in which a local maximum at intermediate activities was found for these

temperatures. In methanol, the position of the local maximum with activity has simply shifted. These results can be explained by solute induced changes of the microphase separation in Nafion. As temperature and solute activity change, the hydrophilic microphase restructures itself. The possible equilibrium phases for Nafion are a disordered phase, a BCC cluster phase, a hexagonal cylindrical phase, and possibly a lamellar phase. For methanol, at intermediate temperature and activity .10, we are in the spherical cluster phase. Since the sulfonic acid groups are phase separated from the TFE in this phase, the TFE's crystalline structure is preserved, and the sample actually creeps less than dry Nafion® at the same temperature. However, as activity is increased further, the microphase evolves into a cylindrical phase and then a lamellar phase, in which more creep occurs due to less phase separation. The results from methanol-water mixtures exhibited a similar result at intermediate temperatures between that of methanol and water, confirming the hypothesis of microphase separation.

Nafion's mechanical properties were also shown to be strongly dependent on thermal history. For the dry Nafion, increased creep strain after drying at higher temperatures is due to the thermal deactivation of S—H cross-links which normally give dry Nafion® its high resistance to creep strain. The lower creep strain for activities 0.10 and 0.65 for the higher drying temperature can be explained in terms of the acid cluster sizes of Nafion. It has been proposed that higher drying temperature results in smaller acid clusters due to denser packing of side and main chains. Smaller clusters will result in a smaller methanol uptake by the membrane, which means less creep will occur for a higher drying temperature. Increasing drying time increased creep. If the membrane is dried for a longer period of time, it does not have time to revert to its ordered state, and more creep occurs.

The final morphology of Nafion is a function of solvent type and activity, temperature, and thermal history. Tensile creep response has been investigated varying all of these factors in order to gain a better understanding of Nafion's morphology under different conditions, and its effect on the polymer's mechanical properties. It was found that all of factors had a significant effect on mechanical properties. Since the mechanical properties of the polymer electrolyte membrane influence the performance, longevity and durability of the fuel cell, it is very important to have a good understanding of these properties under the actual operating conditions of the fuel cell. Further work should investigate how Nafion could be modified to improve its performance under different environmental conditions. Additionally, experiments could be repeated with other solvents in order to gain a better understanding of the theory of microphase separation in Nafion.

This paper represents my own work in accordance with University regulations.

*Christine Ranney*

## References

1. Bauer, F.; Denneler, S.; Willert-Porada, M., Influence of temperature and humidity on the mechanical properties of Nafion (R) 117 polymer electrolyte membrane. *Journal Of Polymer Science Part B-Polymer Physics* **2005**, 43, (7), 786-795.
2. Benziger, J., Bocarsly, A., Majsztrik, P.W., Ranney, C. Solute induced phase transitions in Nafion. Submitted to *Macromolecules* **2008**.
3. Chang H.; Kim J.R.; Cho J.H.; Kim H.K.; Choi K.H. Materials and Processes for Small Fuel Cells. *Solid State Ionics*. **2002**. 148(3), 601-606
4. Duplessix, R.; Escoubes, M.; Rodmacq, B.; Volino, F.; Roche, E.; Eisenberg, A.; Pineri, M., Water-Absorption in Acid Nafion Membranes. *Abstracts of Papers of the American Chemical Society* **1979**, (SEP), 19-19.
5. Elliot, J., Hanna, S. Interpretation of the Small-Angle X-ray Scattering from Swollen and Oriented Perfluorinated Ionomer Membranes. *Macromolecules* **2000**. 33, 4161-4171
6. Fujimura, M.; Hashimoto, T.; Kawai, H. Small-Angle X-Ray-Scattering Study of Perfluorinated Ionomer Membranes .2. Models for Ionic Scattering Maximum. *Macromolecules* **1982**, 15, (1), 136-144.
7. Gierke, T. D.; Munn, G. E.; Wilson, F. C., The Morphology in Nafion Perfluorinated Membrane Products, as Determined by Wide-Angle and Small-Angle X-Ray Studies. *Journal of Polymer Science Part B-Polymer Physics* **1981**, 19, (11), 1687-1704.
8. Hensley, J. E.; Way, J. D.; Dec, S. F.; Abney, K. D., The effects of thermal annealing on commercial Nafion membranes. *Journal of Membrane Science*. **2007**, 298(1-2), 190-201.
9. Hinatsu, J. T.; Mizuhata, M.; Takenaka, H., Water-Uptake Of Perfluorosulfonic Acid Membranes From Liquid Water And Water-Vapor. *Journal Of The Electrochemical Society* **1994**, 141, (6), 1493-1498.
10. Hogarth, M.P.,G.A. Hards. Technological Advances and Further Requirements. *Platinum Metals Review*. **1996**, 40 (4), 150-159
11. Hsu, W. Y.; Gierke, T. D., Ion-Transport and Clustering in Nafion Perfluorinated Membranes. *Journal of Membrane Science* **1983**, 13, (3), 307-326.
12. Jiang, R., Chu, D., Comparative Studies of Methanol Crossover and Cell Performance for a DMFC. *Journal of the Electrochemical Society* **2004**, 151(1), A69-A76.

13. Jones, H. Phelps, E. Hu, M. Microfuel processor for use in a miniature power supply. *Journal of Power Sources* **2002**, 108, 21–27
14. Lamy, C., Lima, A., LeRhun, V., Delime, F., Coutanceau, C., Léger, J.M., Recent advances in the development of direct alcohol fuel cells (DAFC). *Journal of Power Sources*. **2002** 105,283-296.
15. Laporta, M.; Pegoraro, M.; Zanderighi, L., Perfluorosulfonated membrane (Nafion): FT-IR study of the state of water with increasing humidity. *Physical Chemistry Chemical Physics* **1999**, 1, (19), 4619-4628.
16. Lin, J., Lee, J. K., Kellner, M., Wycisk, R., Pintauro, P.N. Nafion-Flourinated Ethylene-Propylene Resin Membrane Blends for Direct Methanol Fuel Cells. *Journal of the Electrochemical Society* **2006**, 153 (7) A1325 .
17. Liu, D.; Kyriakides, S.; Case, S. W.; Lesko, J. J.; Li, Y. X.; McGrath, J. E., Tensile behavior of Nafion and sulfonated poly(arylene ether sulfone) copolymer membranes and its morphological correlations. *Journal of Polymer Science Part B-Polymer Physics* **2006**, 44, (10), 1453-1465.
18. Liu, R., Smotkin, E.S., Array Membrane Electrode Assemblies For High Throughput Screening of Direct Methanol Fuel Cell Catalysts. *Journal of Electroanalytical Chemistry* **2002**, 535, 49-55
19. Majsztrik, P. W. Mechanical and Transport Properties of Nafion® for PEM Fuel Cells; Temperature and Hydration Effects. *Princeton University*. Princeton, **2007**.
20. Majsztrik, P. W.; Satterfield, M. B.; Bocarsly, A. B.; Benziger, J. B., Water Sorption, Desorption and Transport in Nafion Membranes. *Journal of Membrane Science* **2007**, (In press).
21. Majsztrik, P.W. Environmental control chamber for mechanical testing instrumentation accurately controlling temperature, relative humidity and pressure during mechanical tests. 2007.
22. Matsen MW, Bates FS. Unifying weak- and strong-segregation block copolymer theories. *Macromolecules* **1996**, 29(4):1091-1098.
23. Mauritz, K.A.,Moore, R.B., State of understanding of Nafion. *Chemical Review* **2004**, 104 (10), 4535-4585.
24. Miura, Y.; Yoshida, H., Effects of Water and Alcohols on Molecular-Motion of Perfluorinated Ionomer Membranes. *Thermochimica Acta* **1990**, 163, 161-168.
25. Nafion™Membrane: An Infrared Spectroscopy Study. *Fuel Cells* **2007**, 7 (5). 408-416

26. Robertson, M. A. F. Ph.D. Thesis, *University of Calgary*, **1994**.
27. Roche, E. J.; Pineri, M.; Duplessix, R., Phase Separation in Perfluorsulfonate Ionomer Membranes. *Journal of Polymer Science* **1982**, 20, 107-116.
28. Satterfield, M. B. Mechanical and Water Sorption Properties of Nafion® and Nafion®/Titanium Dioxide Membranes for Polymer Electrolyte membrane Fuel Cells. *Princeton University*, Princeton, **2007**.
29. Satterfield, M. B.; Majsztrik, P. W.; Ota, H.; Benziger, J. B.; Bocarsly, A. B., Mechanical Properties of Nafion and Titania/Nafion Composite Membranes for PEM Fuel Cells. *Journal of Polymer Science Part B-Polymer Physics* **2006**, 44, 2327-2345.
30. Scholta, G. Escher, Zhang, L. Küppers, Jörissen, L. and Lehnert W., Investigation on the influence of channel geometries on PEMFC performance, *Journal of Power Sources* **2006**, 155, 66-71
31. Stanic, V, Hoberecht, M. Mechanism of Pinhole Formation in Membrane Electrode Assemblies for PEM Fuel Cells. *NASA Glenn Research Center Report Number E-114868*. 2004
32. Tang, Y. L.; Karlsson, A. M.; Santare, M. H.; Gilbert, M.; Cleghorn, S.; Johnson, W. B., An experimental investigation of humidity and temperature effects on the mechanical properties of perfluorosulfonic acid membrane. *Materials Science and Engineering a-Structural Materials Properties Microstructure and Processing*, **2006**, 425, (1-2), 297-304.
33. Tsai, C.E., Hwang, B.J.. Intermolecular Interactions Between Methanol/Water Molecules and Nafion® Membrane: An Infrared Spectroscopy Study 2007, 7(5), 408-416.
34. Yang, C., Srinivasan, S., Bocarsly, A.B., Tulyani, S., Benziger, J.B. A comparison of physical properties and fuel cell performance of Nafion and zirconium phosphate/Nafion composite membranes, *Journal of Membrane Science* **2004**, 237, 145-161
35. Yeager, H. J.; Eisenberg, A. Perfluorinated Ionomer Membranes; ACS Symp. Ser. No.180, (American Chemical Society: Washington, DC, 1982) 1-6, 41-63.